SUBSTRATE ELASTICITY REGULATES THE BIOPHYSICAL PROPERTIES OF HEMATOPOIETIC STEM AND PROGENITOR CELLS

BY

JI SUN CHOI

THESIS

Submitted in partial fulfillment of the requirements
for the degree of Master of Science in Chemical Engineering
in the Graduate College of the
University of Illinois at Urbana-Champaign, 2011

Urbana, Illinois

Adviser:

Assistant Professor Brendan A. C. Harley

ABSTRACT

Physiological environments of the HSC niches exhibit a range of stiffness, ranging from soft marrow (< 1 Pa) to adipose tissue (1~3 kPa) to non-mineralized bone (> 34 kPa) (Patel, Smith et al. 2005; Engler, Sen et al. 2006; Discher, Mooney et al. 2009). In order to decouple the effects of substrate elasticity, ligand concentration, and dimensionality on hematopoietic stem cell (HSC) fate (quiescence, self-renewal, differentiation, mobilization, homing, and apoptosis), HSCs harvested from C57B6 mouse femurs and tibias were cultured in or on top of collagen hydrogels or on top of 2D polyacrylamide (PA) gels with varying mechanics and ligand densities. With collagen hydrogels and type I collagen-coated PA gels with varying stiffness, simple *in vitro* biomaterials system to probe the effects of substrate mechanics on the biophysical properties of HSCs were created. When cultured for 24 hours, HSCs exhibited varying degrees of changes in their biophysical properties (cell viability, spread area, cell morphology) with increasing substrate stiffness. In general, HSCs spread out more and showed more irregular morphology with increasing substrate elasticity and ligand density. The observed behaviors were different from those of 32D cells, which are further differentiated IL-3 dependent murine myeloid progenitor cells from a cell line, that showed overall much more spread out and amorphous morphology with optimal spreading at an intermediate ligand density.

ACKNOWLEDGMENTS

First and foremost, I want to thank Professor Brendan Harley for his guidance and support. I am especially grateful for him to believe in me when things were not exactly going as planned. Next, I want to thank my lab members (Bhushan, Steven, Dan, Emily, Jackie, Sara, Laura, Rebecca, Tamaki) for making the lab life more enjoyable and bearable. In particular, I want to thank Bhushan Mahadik for friendly conversations, helpful discussions and support. I was one of the first three graduate students to join the lab and it has been my pleasure to see the lab grow in many dimensions. I feel very fortunate to have been a part of this learning process.

I would like to acknowledge two very talented undergraduate students who contributed to my work. Tyler Leonard performed rheological measurements of collagen hydrogels and Roxanne De Leon fabricated polyacrylamide gels. I would also like to thank the following people at the University of Illinois at Urbana-Champaign for their technical assistance. Dr. Barbara Pilas and Ben Montez at the Flow Cytometry Facility of Roy J. Carver Biotechnology Center have been invaluable resources in performing FACS. Dr. Scott Maclaren at the Frederick Seitz Material Research Laboratory has been very helpful and supportive with AFM measurements and analysis. Russell Borduin from Prof. Ning Wang's lab (Dept. of Mechanical Engineering) kindly shared their polyacrylamide gel fabrication protocol. Dr. Sivaguru Mayandi at the Institute for Genomic Biology (IGB) Microscopy Facility has been extremely helpful with imaging work. Prof. Charles F. Zukoski kindly allowed the use of his rheology equipment for collagen hydrogel mechanical characterization.

Last but not least, I would like to thank my family and friends who have always been there for me. Thank you, Mom and Dad as well as my little brother Hong Ik for always believing in me. You guys are the best! Thank you my friends for our lovely times together (You know who you are). It has been quite frustrating and even demoralizing at times to make things work. It truly would not have been the same without you guys. I love you all!

The work described here was funded by American Cancer Society (IL - #160673), the Chemical and Biomolecular Engineering Department, and the Institute for Genomic Biology at the University of Illinois at Urbana-Champaign. This research was carried out in part in the Frederick Seitz Materials Research Laboratory Central Facilities, University of Illinois, which are partially supported by the U.S. Department of Energy under grants DE-FG02-07ER46453 and DE-FG02-07ER46471.

TABLE OF CONTENTS

LIST OF SYMBOLS AND ABBREVIATIONS vii
CHAPTER 1: INTRODUCTION AND BACKGROUND 1
1.1. Hematopoietic stem cells (HSCs) 1
1.2. HSC niches and intrinsic/extrinsic regulation of HSC fate 1
1.3. Clinical importance of HSCs 2
1.4. Mechanical cues in HSC regulation 4
1.5. Determining the role of substrate elasticity on HSC early-fate regulations 5
1.6. Thesis Organization 9
1.7. Statistical analysis 10
1.8. Figures 11
CHAPTER 2: FABRICATION AND MECHANICAL CHARACTERIZATION OF POLYACRYLAMIDE GELS AND COLLAGEN HYDROGELS 14
2.1. Introduction 14
2.2. Collagen hydrogels 14
2.3. Polyacrylamide (PA) gels 16
2.4. Results summary 22
2.5. Figures 24
2.6. Tables 29
CHAPTER 3: HSC CULTURE AND OBSERVED BIOPHYSICAL CHANGES 30
3.1. Introduction 30
3.2. Isolation of HSCs 30
3.3. HSC culture conditions 31
3.4. HSC viability 32
3.5. Biophysical changes observed in HSCs 32
3.6. Discussion 36
3.7. Figures 40
3.8. Conclusions 46
CHAPTER 4: 32D CELL CULTURE AND OBSERVED BIOPHYSICAL CHANGES 47
4.1. Introduction 47
4.2. 32D cell line 47
4.3. 32D cell culture conditions 47
4.4. 32D cell viability 48
4.5. Biophysical changes observed in 32D cells 48
4.6. Discussion 50
4.7. Figures 52
4.8. Conclusions 54
CHAPTER 5: CONCLUSIONS 55
5.1. Conclusions 55
5.2. Future work 55
APPENDIX A: GEL FABRICATION AND CHARACTERIZATION PROTOCOLS 57
A.1. Collagen hydrogel fabrication protocol 57
A.2. Collagen hydrogel cell encapsulation protocol 58
A.3. SEM imaging of collagen hydrogel protocol 59
A.4. Collagen hydrogel mechanical characterization protocol 60

A.5. PA gel fabrication protocol 61
A.6. PA gel surface functionalization protocol 63
A.7. PA gel collagen-coating quantification protocol 64
A.8. AFM force measurement protocol 65
APPENDIX B: CELL CULTURE AND ANALYSIS PROTOCOLS 69
B.1. HSC isolation protocol 69
B.2. Cell viability assay protocol 72
B.3. Fixed cell staining protocol 73
B.4. ImageJ: Cell spread area calculation protocol 74
REFERENCES 76

LIST OF SYMBOLS AND ABBREVIATIONS

Abbreviation	Term, Definition
***α* (alpha)**	Opening angle of the tip
AFM	Atomic force microscopy
ANOVA	One-way analysis of variance
BM	Bone marrow
CAR cells	CXCL12-abundant reticular (CAR) cells
CFC/CFU	Colony forming cells/ Colony forming units
CLP	Common lymphoid progenitor
CMP	Common myeloid progenitor
CSI	Cell shape index
CXCL12	(C-X-C motif) ligand 12
***δ* (delta)**	Indentation
d	Deflection of the cantilever
d_0	Zero deflection
DC	Dendritic cell
DCDMS	Dichlorodimethylsilane
E	Elastic modulus
ECM	Extracellular matrix
ESC	Embryonic stem cell
F	Loading force
FACS	Fluorescence-activated cell sorting
G-CSF	Granulocyte-colony stimulating factor
GMP	Granulocyte-monocyte progenitor
HSC	Hematopoietic stem cell
HSPC	Hematopoietic stem and progenitor cell
IL	Interleukin
k	Force constant of the cantilever
LSK cells	$Lin^-Sca\text{-}1^+c\text{-}Kit^+$ population
LT-HSC	Long-term hematopoietic stem cell
MC3T3-E1	Mouse pre-osteoblast cell line
MEP	Megakaryocyte-erythrocyte progenitor
ML-7	myosin light chain kinase
MPP	Multipotent progenitor
MSC	Mesenchymal stem cell
NK cell	Natural Killer cell
***ν* (nu)**	Poisson ratio
PA	Polyacrylamide
SCF	Stem cell factor
SDF-1	Stromal cell-derived factor-1
SEM	Scanning electron microscope
SEM	Standard error of the mean
ST-HSC	Short-term hematopoietic stem cell
TEMED	Tetramethylethylenediamine
TPO	Thrombopoietin

VCAM-1	Vascular cell adhesion molecule-1
VLA-4	Very late antigen-4
z	Piezo movement in the z direction
z_0	Contact point

CHAPTER 1: INTRODUCTION AND BACKGROUND

1.1. Hematopoietic stem cells (HSCs)

Hematopoietic stem cells (HSCs) are adult stem cells that reside primarily in the bone marrow with the capacity to give rise to all cells of myeloid (erythrocytes, platelets, granulocytes, macrophages, etc.) and lymphoid (T cells, NK cells, B cells, etc.) lineages, as shown in **Figure 1.1**. A hierarchical system of HSCs and progenitor cells exists, differing in their ability to reconstruct the bone marrow. Long-term HSCs (LT-HSCs) can engraft lethally-irradiated bone marrow for at least 6 months while short-term HSCs (ST-HSCs) can only do so for up to 3 months with limited self-renewal capacity. Most further differentiated forms of progenitors cannot self-renew and are committed to give rise to specific cell types only (Zon 2008).

1.2. HSC niches and intrinsic/extrinsic regulation of HSC fate

Stem cells are housed in a specialized microenvironment known as the stem cell niche, which provides intrinsic and extrinsic signals to regulate their fate: quiescence, self-renewal, differentiation, mobilization, homing, and apoptosis (Wilson and Trumpp 2006; Can 2008). During homeostasis, quiescent HSCs are found at the endosteum (‘endosteal niche’) lined by osteoblasts and nestin-expressing mesenchymal stem cells (MSCs) that supply factors (CXCL12, SCF, Ang-1, VACM-1, and TPO) essential for HSC maintenance. More actively cycling HSCs are located near the center of the bone marrow or in the ‘perivascular niche,’ where they are associated with CXCL12-abundant reticular (CAR) cells, perivascular MSCs, and sinusoidal endothelium. Recently, macrophages were discovered to be positive regulators of osteoblasts and

nestin-expressing MSCs, thereby modulating HSC fate (Ehninger and Trumpp 2011). A schematic of the HSC niches is shown in **Figure 1.2.** HSCs mobilize and circulate into blood streams after a traumatic injury. Signaling molecules such as CXCL12 (SDF-1) and BIO5192 (antagonist to VCAM-1 /VLA-4 niche interaction) have been found to be able to cause HSC mobilization *in vivo.* Alternatively, injection of Granulocyte-colony stimulating factor (G-SCF) can be used to induce HSC mobilization from the niches (Ross and Li 2009).

Like this, various types of cells that are in close proximity to HSCs along with soluble factors (growth factors, chemokines, ligands, etc.) present in the niches have been identified to modulate HSC fate and maintenance by mediating paracrine signaling and other molecular level pathways. Notably, developmental pathways such as Wnt and NOTCH signaling pathways have been discovered to be involved with HSC self-renewal. In addition, epigenetic regulation via chromatin-associated factors (e.g. Bmi1), cell-cycle regulators (e.g. PTEN), and blood transcription factors (e.g. *GATA2*) has also been found to be an integral part of maintaining a healthy HSC pool (Wilson and Trumpp 2006; Zon 2008). ECM components (ECM proteins and ECM mechanical properties) have also been found to influence different types of stem cells (Discher, Mooney et al. 2009), although their effects on HSCs have not yet been elucidated.

1.3. Clinical importance of HSCs

Every year, a large number of people develop and/or suffer from bone marrow and blood-derived cancers and diseases. These include leukemia, a type of cancer affecting the blood and bone marrow, lymphoma, a type of cancer affecting the lymphatic system, and myeloma, a type of

cancer affecting the plasma cells of the marrow. Each year, approximately 750,000 people in the United States are suffering or in remission from one of these potentially fatal conditions. Relapse after recovery is not uncommon. Incidence rates of cancers typically increase with age, thus the number of people diagnosed with such conditions is expected to rise as the overall population grows older with improved life expectancy (lls.org 2011; Ped-Onc.org 2011).

Treatment options vary but usually include extensive chemotherapy, drug therapies, and stem cell transplantation. Transplantation of functional HSCs harvested from the patient body ('autologous transplantation') would be ideal; however, there are limitations because no well-established protocols currently exist to effectively expand functional HSCs *in vitro* or *in vivo* without having any adverse effects. HSCs are rare and thus account for only 0.5% the whole bone marrow population (Wilson and Trumpp 2006; lls.org 2011).

Recent evidence suggests that a small population of cancer-causing 'leukemic stem cells' may exist (Bonnet and Dick 1997; Jan, Chao et al. 2011). These are thought to be normal HSCs that have been turned malignant due to genetic or other events still unknown. The presence of such malignant stem cells with long-term self-renewal potential may be the reason why relapse occurs. On the other hand, it has also been proposed that a population of healthy HSCs still exists in patients with leukemia, as evidenced by the occurrence of normal hematopoiesis upon the injection of their stem cells into lethally irradiated mice (Taussig, Miraki-Moud et al. 2008). The existence of 'cancer stem cells' has also been postulated for other types of cancers including human brain tumors (Singh, Clarke et al. 2003), pancreatic cancers (Li, Lee et al. 2009), and prostate cancers (Collins, Berry et al. 2005).

Understanding the biological mechanisms of HSC maintenance and regulation would therefore not only elucidate the pathology of the blood and bone marrow-derived cancers and hence provide useful and improved treatment options, but also benefit the field of cancers by contributing to the understanding of cancers in general.

1.4. Mechanical cues in HSC regulation

Unlike cell-cell interactions, the role of mechanical cues in HSC fate regulation has not been considered until recently. Holst *et al.* observed that mouse whole bone marrow cells were enriched in HSC population ($Lin^{-}Sca\text{-}1^{+}c\text{-}Kit^{+}$) by up to 14.2-fold when they were cultured on tropoelastin-coated well-plates. This effect was not seen when the mechanosensing ability of the cells were masked by inhibiting myosin II heavy chain (blebbistatin) and myosin light chain kinase (ML-7) or when the effects of tropoelastin were negated via treatment with glutaraldehyde, thus highlighting the significance of 'substrate tensegrity' in HSC regulation (Holst, Watson et al. 2010).

Recent studies with MSCs suggest that the mechanical properties of the extracellular matrix (ECM) play an important role in determining stem cell fate. Human MSCs were found to selectively take neurogenic, myogenic or osteogenic differentiation pathways when they were cultured on collagen-coated polyacrylamide (PA) gels with varying stiffness mimicking the stiffness of the brain (0.1 – 1 kPa), muscle (8 – 17 kPa) or the collagenous bone (25 – 40 kPa) (Engler, Sen et al. 2006). Similarly, myogenic commitment of MSCs was optimized on 25-kPa

and 80-kPa PA gels coated with fibronectin and type I collagen, respectively (Rowlands, George et al. 2008). Substrate modulus was also found to regulate neural stem cell behavior, favoring neural differentiation on soft substrates (100 – 500 Pa) and glial cultures on stiff substrates (1 – 10 kPa) (Saha, Keung et al. 2008). Thus, ECM mechanics as well as the presentation of ECM proteins seem to influence stem cell behaviors.

1.5. Determining the role of substrate elasticity on HSC early-fate regulations

Although Holst *et al.* showed the importance of 'substrate tensegrity' on HSC expansion via mechanotransduction, other aspects of the HSC niches – substrate elasticity, dimensionality, ligand density, and ligand presentation – have not been considered until now. Understanding the relationship between such factors and HSC behaviors would be critical in elucidating the underlying mechanisms by which HSCs are regulated in their niche microenvironments in order to supply all of the blood and immune cells for the life span of an animal.

The aim of this study is to decouple the effects of substrate elasticity, ligand concentration, and dimensionality on HSC fate by culturing HSCs in or on top of collagen hydrogels or on top of 2D PA gels with varying mechanics and ligand densities. Physiological environments of the HSC niches exhibit a range of stiffness, ranging from soft marrow (< 1 Pa) to adipose tissue (1~3 kPa) to non-mineralized bone (> 34 kPa) (Patel, Smith et al. 2005; Engler, Sen et al. 2006; Discher, Mooney et al. 2009). With collagen hydrogels and type I collagen-coated PA gels with varying stiffness, simple *in vitro* biomaterials system to probe the effects of substrate mechanics on the

biophysical properties of HSCs were created. The range of stiffness observed in HSC niches are summarized in **Figure 1.3.** The schematic of the experimental setup is depicted in **Figure 1.4.**

1.5.1. Choice of biomaterials

Physiological environments of the HSC niches exhibit a range of stiffnesses, ranging from soft marrow (< 1 Pa) to adipose tissue (1~3 kPa) to non-mineralized bone (> 34 kPa) (Patel, Smith et al. 2005; Engler, Sen et al. 2006; Discher, Mooney et al. 2009). It was therefore desirable to choose a biomaterial whose elastic modulus could be tuned over a wide range of stiffness. It was also critical that the biomaterial can be easily functionalized with various ECM proteins to present ligands. In addition, the biomaterial had to be non-cytotoxic in order to encapsulate cells to provide 3D microenvironments. To meet such requirements, polyacrylamide (PA) gels and collagen hydrogels have been chosen to serve as a biomaterials platform. PA gels are useful for providing 2D culture environments with tunable mechanics over a broad range while collagen hydrogels are advantageous for soft 3D culture environments.

1.5.1.1. Polyacrylamide (PA) gels

Polyacrylamide (PA) is a polymer (-$CH_2CHCONH_2$-) that is synthesized from crosslinking acrylamide and bisacrylamide monomers. It has many advantages which make it a popular choice for cell studies such as traction, spreading, and migration studies. First of all, it is non-toxic and is highly water absorbent. It is also clear, which allows for convenient brightfield and fluorescence imaging. For this purpose, it can be made as a thin and flat 2D gel (< 100 μm thickness) that is covalently attached to a glass substrate underneath it. Most importantly, its mechanical properties can be easily tuned by varying the concentrations of the acryladmie and

bisacrylamide monomers. Resulting PA gels range from very soft (< 1 kPa) to stiff (> 100 kPa) gels. Its surface can also be modified to react with primary amine groups of a protein via UV-crosslinking of Sulfo-SANPAH, a heterobifunctional photoreactive reagent which is employed to coat the PA gel surface with a protein of choice in order to facilitate cell attachment. One major drawback of using the PA gels for cell cultures is that the PA gels cannot be made as 3D constructs to have the cells embedded inside (Pelham and Wang 1997; Beningo, Lo et al. 2002; Kandow, Georges et al. 2007).

1.5.1.2. Collagen hydrogels

Collagen is a major ECM protein that is an integral part of the connective tissues and many other types of tissues such as bone, skin, tendon, ligament, and cartilage. Various types of collagen have been identified, but type I collagen is most abundant in the bone, where HSC niches are located. Collagen-based biomaterials such as collagen scaffolds have been widely used in tissue engineering applications due to a number of useful properties: requisite hemostatic properties, low antigenicity, and appropriate mechanical characteristics (Yannas, Tzeranis et al. 2010).

Collagen hydrogels, on the other hand, are fabricated typically from diluting type I collagen with the respective culture medium and inducing polymerization through incubation at an elevated temperature (Baker, Bonnecaze et al. 2009). They are easy to fabricate and can provide very soft (< 1 kPa) culture environments. It is also possible to make them stiffer to a certain degree by increasing the collagen concentration or by adding in other elements (e.g. hyaluronan) that could give additional structural support (Yang and Kaufman 2009). A major advantage with collagen hydrogels is that cells can be encapsulated inside in order to provide 3D culture conditions.

1.5.2. Choice of cell types

Two types of cells – HSCs and 32D cells – have been chosen for this study.

1.5.2.1. HSCs

Because no cell lines have been established for HSCs, primary cells that are harvested directly from animals must be used. Primary murine HSCs from femurs and tibias of C57B6 mouse are therefore chosen. HSCs are collected via fluorescence-activated cell sorting (FACS). Several cell surface antigens have been identified for the primitive HSC population. LSK ($Lin^-Sca\text{-}1^+c\text{-}Kit^+$) population is often used to distinguish HSPCs from other committed cell types (Weissman and Shizuru 2008). Thus, this population of HSCs was chosen for the HSC experiments.

1.5.2.2. 32D cells

In order to compare HSC behavior with a more committed cell population, 32D cells were used as a control. 32D cells are interleukin-3 (IL-3) dependent murine myeloid progenitor cells that are widely used as an *in vitro* model of hematopoiesis. They terminally differentiate into neutrophilic granulocytes upon the removal of IL-3 and injection of granulocyte-colony stimulating factor (G-CSF) to the culture medium, and this differentiation process closely resembles the differentiation patterns inside the marrow (Valtieri, Tweardy et al. 1987; Agliano, Santangelo et al. 2000). For this reason, 32D cells are often employed as a model system for hematopoiesis.

1.6. Thesis Organization

The thesis is organized in the flowing manner:

† Chapter 2 provides fabrication of collagen hydrogels and PA gels and subsequent mechanical characterization of these gels via rheology and atomic force microscopy (AFM).

† Chapter 3 presents the biophysical changes observed (changes in cell morphology, % cell viability, spread area, cell shape index (CSI)) when HSCs were cultured on top of fabricated PA gels and on top of or inside collagen hydrogels for 24 hours.

† Chapter 4 shows the biophysical changes observed in 32D cells when they were cultured on top of fabricated PA gels and on top of or inside collagen hydrogels for 24 hours.

† Chapter 5 summarizes and concludes findings while providing directions for future work, which can build upon the results of the present work.

† Appendix A includes protocols for collagen hydrogel and PA gel fabrication and their characterization. Appendix B presents protocols for HSC culture and analysis.

1.7. Statistical analysis

One-way analysis of variance (ANOVA) with Tukey test was performed in OriginPro (Origin Lab Corp., Northampton, MA) to determine statistical differences between data groups. For all figures, standard error of the mean (SEM) was drawn as error bars. Standard deviation was used for the elastic moduli of the PA gels.

1.8. Figures

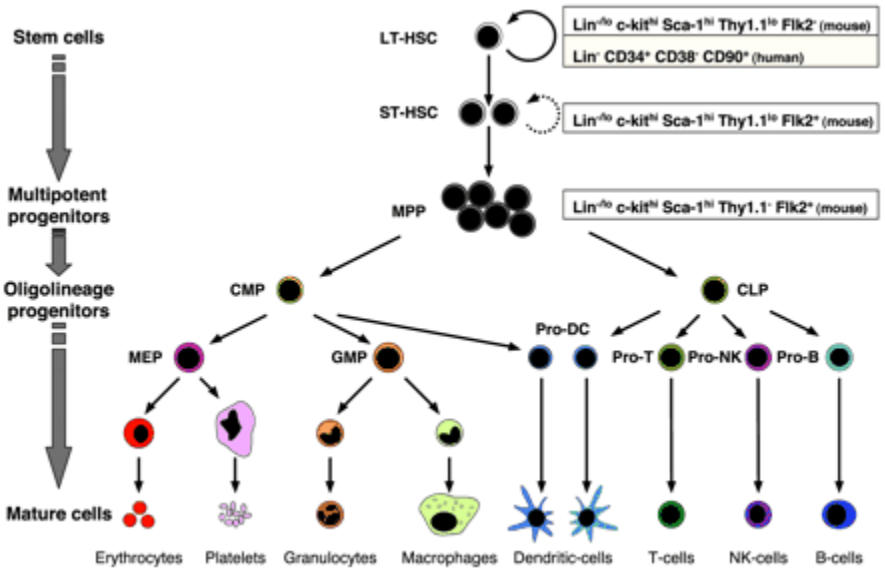

Figure 1.1. HSC lineages, showing highly primitive LT-HSCs which can reconstitute an animal indefinitely, ST-HSCs which can reconstitute an animal with limited self-renewal capacity, MPPs and other progenitors (CMP, CLP, MEP, GMP, etc.) which are further restricted in their self-renewal potential, and terminally differentiated cells. LT-HSC: Long-term HSC; ST-HSC: Short-term HSC; MPP: Multipotent progenitor; CMP: Common myeloid progenitor; CLP: Common lymphoid progenitor; MEP: Megakaryocyote-erythrocyte progenitor; GMP: Granulocyte-monocyte progenitor (Passegue, Jamieson et al. 2003).

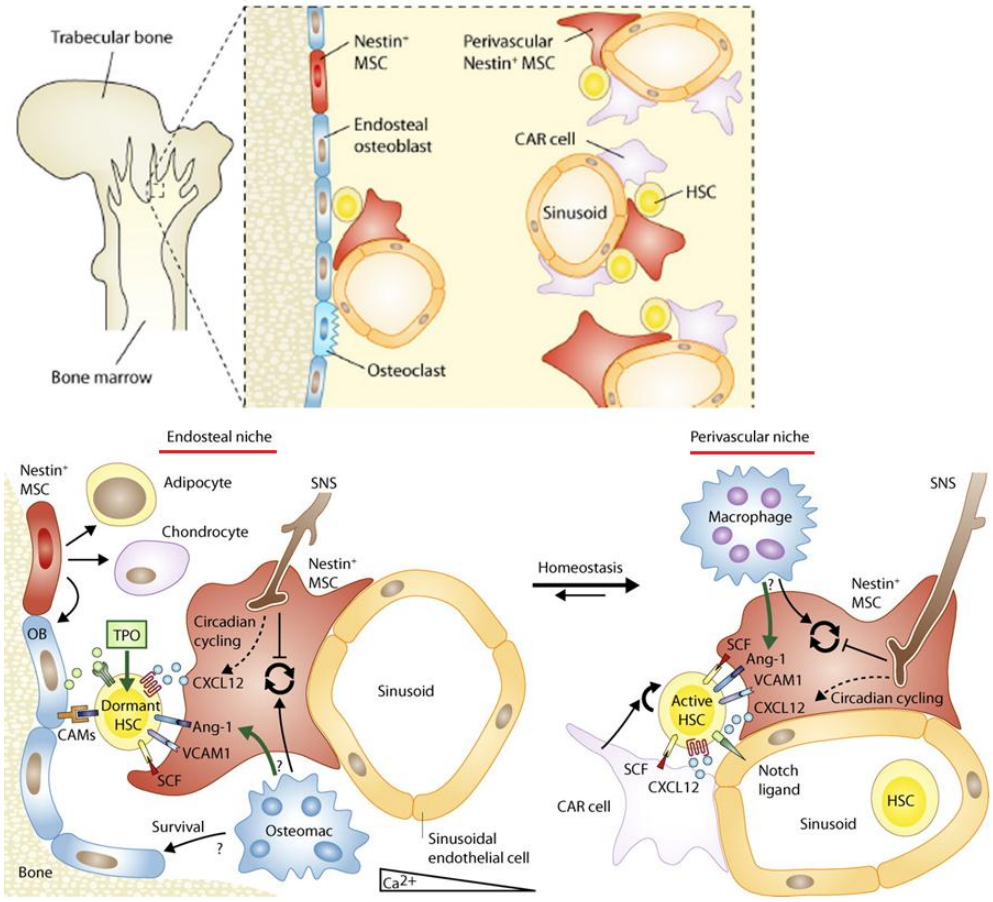

Figure 1.2. Endosteal niche, which is near the endosteum, is lined by osteoblasts and nestin-expressing MSCs while perivascular niche is associated with sinusoidal endothelium and CAR cells (Ehninger and Trumpp 2011).

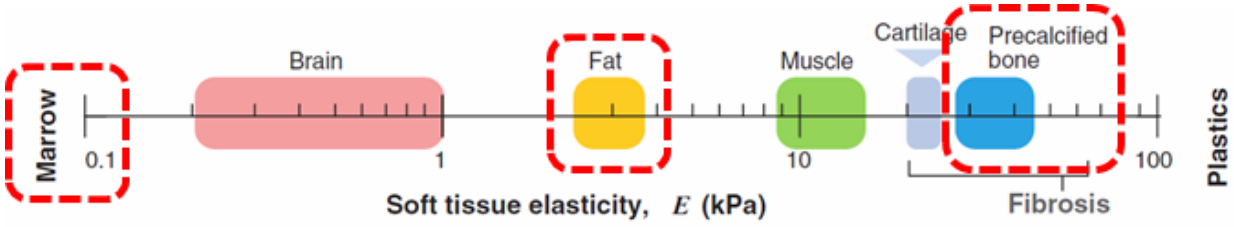

Figure 1.3. A range of stiffness observed in soft tissues. Those that are relevant to HSC niches are highlighted in red dashes (Discher, Mooney et al. 2009).

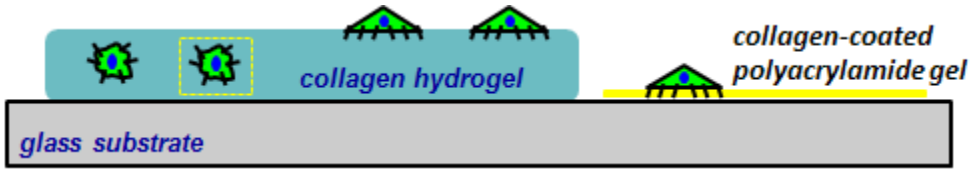

Figure 1.4. Schematic of the proposed experimental design. Cells are to be cultured either on top of 2D hydrogel substrates or encapsulated inside 3D hydrogel constructs to observe changes in their biophysical properties and to elucidate the resulting effects on HSC fate decision processes.

CHAPTER 2: FABRICATION AND MECHANICAL CHARACTERIZATION OF POLYACRYLAMIDE GELS AND COLLAGEN HYDROGELS

2.1. Introduction

The aim of this study is to decouple the effects of substrate elasticity, ligand concentration, and dimensionality on HSC fate (quiescence, proliferation, differentiation, mobilization, homing, apoptosis) by culturing HSCs in or on top of collagen hydrogels or on top of 2D PA gels with varying mechanics and ligand densities. Therefore, collagen hydrogels and PA gels were fabricated and mechanically characterized prior to performing any cell culture experiments.

2.2. Collagen hydrogels

Collagen hydrogels, whose mechanical properties can be tuned based on polymerization temperature, polymerization pH, collagen density, and crosslinking of the collagen fibrils (Raub, Suresh et al. 2007), were created to give soft (< 1 kPa) 2D or 3D culture environments for HSCs and 32D cells. The mechanics of collagen hydrogels were determined using rheology. This section describes the fabrication and mechanical characterization methods employed for collagen hydrogels. Resulting mechanical data is summarized in **Section 2.4.**

2.2.1. Fabrication of collagen hydrogels

Collagen gels were fabricated with type I collagen from rat tail (BD Biosciences, Bedford, MA) according to protocols published elsewhere (Baker, Bonnecaze et al. 2009; Yang and Kaufman 2009). In brief, collagen stock solution (8.25 mg/mL to 9.33 mg/mL) was diluted with the corresponding culture medium to a final concentration of 1.45 or 2.9 mg/mL. To bring the pH to

7.4, 50 μL of 1 M HEPES buffer and appropriate amounts of 0.4 M NaOH were added to the collagen mixture according to previously established calibration curves (data not shown). The solution was placed on a 10-mm or 14-mm glass bottom dish (MatTek Corp., Ashland, MA) and was incubated for at least 2 hours in a humidified 37 ℃ incubator for complete polymerization before cells were seeded on top. Alternatively in order to encapsulate cells inside these gel constructs, a cell suspension containing the desired number of cells was added to the collagen hydrogel mixture in place of the cell-free culture medium at the start of the culture. All reagents required for collagen gel fabrication were pre-cooled to 4 ℃ before use to prevent any premature collagen gelation upon mixing. Refer to **Appendices A.1.** and **A.2.** for more details.

2.2.2. Imaging of collagen hydrogels via scanning electron microscope (SEM)

Fabricated collagen gels were imaged with scanning electron microscope (SEM). Due to their extremely soft nature, the hydrogels had to be snap frozen with liquid nitrogen and freeze dried prior to imaging. Snap freezing with liquid nitrogen protected the collagen fiber structures from being destroyed before the freeze drying step. A complete protocol in taking SEM images is outlined in **Appendix A.3.** SEM images revealed detailed crosslinked collagen fiber structures, as can be seen in **Figure 2.1.** Differences in the microstructure (i.e. pore size) are observed from the SEM images based on the collagen concentration of the gels. Stiffer collagen hydrogels showed smaller pores due to higher levels of collagen fiber crosslinking. In other words, the stiffness of collagen hydrogels increased with increasing levels of crosslinking.

2.2.3. Mechanical characterization of collagen hydrogels

The elastic moduli of collagen gels were determined with the Bohlin C-VOR rheometer (Malvern Instruments, Westborough, MA) in oscillatory mode with a fixed frequency of 1 Hz and an applied strain of 1%. A small volume of collagen gel mixture (350 μL) was first prepared as described in the section **2.2.1** then placed on a 25 ℃ rheometer stage, below a 4° 20-mm cone geometry with a solvent trap. The cone was then lowered to a pre-determined height (150 μm) and excess collagen around the cone was removed. Using the built-in temperature control system, the temperature of the stage was raised to 37 ℃ to induce faster polymerization. The Bohlin software was then set up to perform a three-minute oscillatory test at every twenty-minute interval for a total of 12 hours to determine the kinetics of collagen gelling. The test was set to run only intermittently in order to minimize any disturbance on the fibrillar networks of the collagen fibers. Data were then plotted, and the elastic moduli of the equilibrated regions were averaged to yield the mean elastic moduli of the collagen gels. Data from one such trial is shown in **Figure 2.2.** Details of rheological measurement procedures are presented in **Appendix A.4.**

2.3. Polyacrylamide (PA) gels

Polyacrylamide (PA) gels were fabricated to serve as 2D substrates for cell cultures. Although they cannot serve as 3D constructs, they provided 2D substrates over a wide range of stiffness (~1 kPa - ~200 kPa). PA gels were fabricated according to published protocols (Pelham and Wang 1997; Tse and Engler 2010) and probed with AFM to characterize their mechanics. Resulting mechanical data is summarized in **Section 2.4.**

2.3.1. Fabrication of PA gels

PA gels were fabricated according to published protocols (Pelham and Wang 1997; Tse and Engler 2010). Briefly, the glass microwell of a 14-mm glass bottom culture dish (MatTek Corp., Ashland, MA) was reacted with NaOH and subsequently aminosilanized with 3-aminopropyltrimethoxysilane. A solution of acrylamide/bis-acrylamide was prepared by mixing acrylamide and bis-acrylamide at varying concentrations and adding ammonium persulfate (1/200 v/v) and tetramethylethylenediamine (1/2,000 v/v) to induce polymerization. This solution was placed on top of the silanized glass microwell. A pre-chlorosilanized 12-mm circular coverslip (Fisher Scientific, Pittsburgh, PA) was placed on top of the mixture to ensure the formation of an even gel surface. For complete polymerization, the dish was incubated for 30 minutes at 37 ℃. The coverslip was then carefully removed and the gel was rinsed thoroughly with deionized water. Using this fabrication technique, PA gels with the following acrylamide (v/v %)/bis-acrylamide (v/v %) concentrations were created: 4/0.03, 5/0.1, 5/0.26, 10/0.3 and 38/2. Fabricated PA gels were stored at 4 ℃ until needed. For more detailed procedures, please refer to **Appendix A.5.**

A schematic of the chemistry behind the PA polymerization reaction is shown in **Figure 2.3.** Ammonium persulfate is a strong oxidizing agent that generates free oxygen radicals. Tetramethylethylenediamine (TEMED) is a catalyst that stabilized free radicals and facilitate polymerization. Photoinitiators such as Irgacure 2959 can alternatively be used to induce PA gel polymerization (Pelham and Wang 1997; Kandow, Georges et al. 2007; Tse and Engler 2010).

2.3.2. PA gel surface functionalization with type I collagen

PA gels can be functionalized with any proteins with primary amine groups. For the purpose of this study, PA gels were coated with type I collagen via UV crosslinking. First, Sulfo-SANPAH (Fisher Scientific, Pittsburgh, PA) solution was placed on top of the gels. The gels were then exposed to UV (365 nm) for 6 minutes and rinsed twice with 50 mM HEPES, pH 8.5. This procedure was repeated one more time before type I collagen from rat tail (BD Biosciences, Bedford, MA) at a desired concentration (100 μg/mL, 40 μg/mL, or 1 ng/mL dissolved in 50 mM HEPES, pH 8.5) was deposited on the surface of the activated gels. Collagen solution was left to react with the PA gels overnight at 4 ℃. Prior to use, PA gels were rinsed with PBS and sterilized with UV for 30 minutes. Protocol for PA gel surface protein conjugation is found in **Appendix A.6.**

The detailed chemistry of conjugation through Sulfo-SANPAH is outlined in **Figure 2.4.** It contains a phenylazide group at one end that reacts nonspecifically with PAgel when photoactivated, and a sulfosuccinimidyl group at the other end that reacts selectively with primary amine groups. This reaction requires photoactivation with UV and a pH of 8.5 (i.e. HEPES buffer at pH 8.5) for conjugation reaction to occur. Because most cell culture mediums are at the physiological pH of 7.4, it can be ensured that no further reaction occurs once the protein conjugation step is completed (Kandow, Georges et al. 2007; Tse and Engler 2010).

2.3.2.1. Quantification of the PA gel collagen-coating

As outlined in **Appendix A.7.**, conjugation of type I collagen on PA gel surface was quantified via immunofluorescence as previously reported (Engler, Bacakova et al. 2004; Engler, Richert et

al. 2004). Specifically, 200 µL of 1 ng/mL, 40 µg/mL, and 100 µg/mL type I collagen solutions were deposited onto 14-mm glass bottom culture dishes and left to dry overnight. These corresponded to 12.9922, 5.1969, and 0.0001 µg/cm^2. The next day, these collagen-deposited substrates were incubated in 2% BSA in PBS for 45 minutes to block nonspecific binding. After carefully rinsing with PBS, the dishes were incubated with primary collagen antibody (Abcam, Cambridge, MA) for 1 hr and with Alexa Fluor® 568 secondary antibody (Invitrogen, Carlsbad, CA) for 45 minutes. The samples were rinsed with PBS and imaged with LSM 710 (Carl Zeiss AG, Thornwood, NY) to create a calibration of the fluorescence intensity with varying type I collagen concentration (**Figure 2.5.A.**). Rinsing steps potentially washing away deposited collagen was assumed to be negligible.

Collagen-coated PA gels were prepared for immunofluorescence the same way and imaged to compare with the calibration curve to establish the amount of the cross-linked collagen. The resulting curve is shown in **Figure 2.5.B.**, and the amount of surface-bound collagen was 0.024, 0.489, and 1.364 µg/cm^2 for 1 ng/mL, 40 µg/mL, and 100 µg/mL collagen solutions used. Throughout this thesis, amounts of collagen deposited on PA gels will be referred by the collagen solution (amount/volume) used.

2.3.3. Mechanical characterization of PA gels

Atomic force microscopy (AFM) was used to generate force-indentation curves at multiple contact points (N = 15) on PA gel substrates (N = 2-3) in order to determine substrate elastic moduli. AFM is a powerful and versatile technique that can be used to study soft gels and biological samples via imaging and/or force measurement. It provides topographical images at nanoscale resolution or allows the exertion of small forces (nN scale) on samples, with a power

to scan molecular level samples such as DNA or binding force between single molecules (Domke and Radmacher 1998). For purposes of PA gel mechanical characterization, AFM was used as a nanoindenter measuring the elastic properties of the PA gel samples.

Briefly, AFM MFP-3D manufactured by Asylum Research (Santa Barbara, CA) was used, with PA gels pre-soaked in deionized water till saturation. A silicon nitride probe with a pyramidal tip and a nominal spring constant of 0.06 N/m (DNP-S10; Bruker Corp., Camarillo, CA) was used to make 2-μm indentations on the PA gel surface in liquid contact mode. Resulting force-indentation plots were saved for post analysis. **Appendix A.8.** details procedures for using AFM to take force measurements. Force profiles were collected and fitted with the Hertz cone model to compute the elastic moduli of the corresponding PA gels. **Figure 2.6.** shows an example of the saved force curve.

2.3.3.1. Hertz model to calculate Young's moduli of PA gels

For a conical tip indenting a flat sample, Sneddon's formula for the Herz model with a conical tip shape can be used (Radmacher 1997; Mahaffy, Shih et al. 2000; Gavara and Chadwick 2010) to describe the relationship between the loading force F and the indentation δ, which is given by:

$$F = \left(\frac{2}{\pi}\right)\left[\frac{E}{(1-\nu^2)}\right]\delta^2 \tan\alpha \qquad \textbf{(Equation 2.1.)}$$

where E is the Young's modulus, ν is the Poisson ratio, and α is the opening angle of the tip.

By assuming Hooke's law, which states that the loading force *F* is directly proportional to the deflection of the cantilever (*d*) by a factor of *k* or the force constant of the cantilever, the following equation can be obtained:

$$F = kd = k(z - \delta)$$ (**Equation 2.2.**)

For samples other than an infinitely stiff sample where $d = z$, the deflection of the cantilever (d) can be found by subtracting indentation (δ) from the piezo movement in the z direction (z) (Domke and Radmacher 1998; Carl and Schillers 2008).

By combining these two equations and applying it to the obtained force curve, it is possible to calculate Young's modulus via the following resulting equation:

$$z - z_0 = d - d_0 + \sqrt{\frac{k(d-d_0)}{\left(\frac{2}{\pi}\right)\left[\frac{E}{(1-\nu^2)}\right]\delta^2 \tan\alpha}}$$ (**Equation 2.3.**)

where d_0 is the zero deflection and z_0 is the contact point (Domke and Radmacher 1998). Two data points (d_1, z_1) and (d_2, z_2) defining a range of analysis can be assigned as shown in **Figure 2.7.** for this purpose.

Although geometry is different, AFM force measurements with a pyramidal-shaped AFM tip touching a flat surface (i.e. thin gel) can be approximated using the Hertz model described above. Sharp tips (pyramidal shape) may result in slightly higher Young's moduli than conical tips when the same samples are probed (Carl and Schillers 2008).

Using the Hertz cone model, elastic moduli of three different PA gels with the following acrylamide (v/v %)/bis-acrylamide (v/v %) concentrations (v/v%) were calculated: 5/0.1, 5/0.26, and 38/2. These values were well-correlated with previously reported data (Tse and Engler 2010). To assess the effect of collagen-coating on the substrate stiffness, PA gels (38%/2%) were coated with three different collagen-coating densities (100 μg/mL, 40 μg/mL, or 1 ng/mL) and tested with AFM. There were no statistical differences between these samples (**Figure 2.8**).

2.4. Results summary

Rheological measurements of the collagen hydrogels revealed their polymerization kinetics, which showed a rapid polymerization phase that took place for the first two hours. The elastic moduli of the collagen hydrogels remained stable once this initial polymerization phase was complete (**Figure 2.2.**). The averaged elastic moduli of the two collagen hydrogels (1.45 mg/mL; 2.9 mg/mL) used in cell cultures are shown in **Table 2.1.**

Elastic moduli of the three fabricated PA gels (acrylamide (v/v %)/bis-acrylamide (v/v %) concentrations: 5/0.1, 5/0.26, and 38/2) were computed from force indentation curves acquired via AFM. The Poisson ratio (ν) was assumed to be 0.4, which is within the published range of ν = 0.3 – 0.5 for PA gels (Engler, Bacakova et al. 2004). The calculated elastic moduli were well-correlated with previously reported values (Tse and Engler 2010); thus, all other PA gels (i.e. 4%/0.03%) fabricated were assumed to hold moduli as previously published. In summary, the fabricated PA gels had Young's moduli ranging from 0.71 kPa to 196 kPa (**Table 2.2.**).

The effect of collagen conjugation and collagen-coating density on PA gel stiffness was assessed by comparing the elastic moduli of the same PA gels (196 ± 54.1 kPa) left uncoated with those coated with three different collagen densities (100 μg/mL, 40 μg/mL, or 1 ng/mL). There were no statistical differences ($P > 0.05$) between uncoated and coated samples, as well as between samples coated with varying collagen concentrations. Therefore, collagen coating and coating density had negligible effects on PA substrate elasticity.

Collagen conjugation on PA gel surface was verified and quantified with immunofluorescence. The amounts of collagen bound to the PA gel surface were 0.024, 0.489, and 1.364 μg/cm^2 for 1 ng/mL, 40 μg/mL, and 100 μg/mL collagen solutions used. Throughout this thesis, amounts of collagen deposited on PA gels will be referred by the collagen solution (amount/volume) used.

2.5. Figures

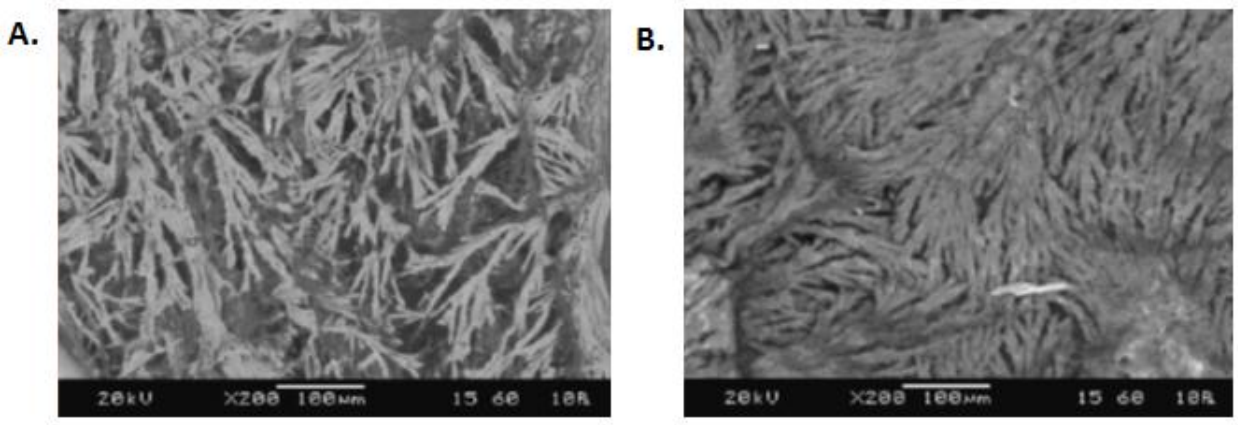

Figure 2.1. Collagen hydrogels at 1.45 mg/mL (A) and 2.9 mg/mL (B) were imaged with SEM at 200x magnification. The gels were snap frozen in liquid nitrogen and freeze dried at -4 ℃ for 18 hours prior to imaging.

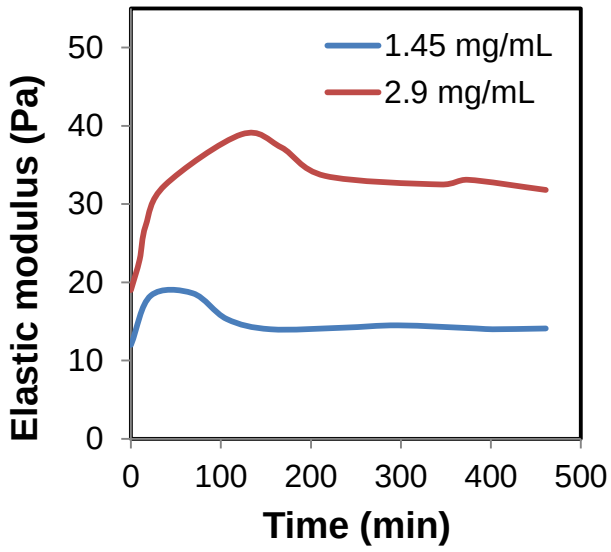

Figure 2.2. Elastic moduli of collagen hydrogels measured from rheology were plotted vs. time. The gelation kinetics shows that the elastic modulus was saturated and plateaued between 1.5 and 2 hours from when the polymerization was initiated.

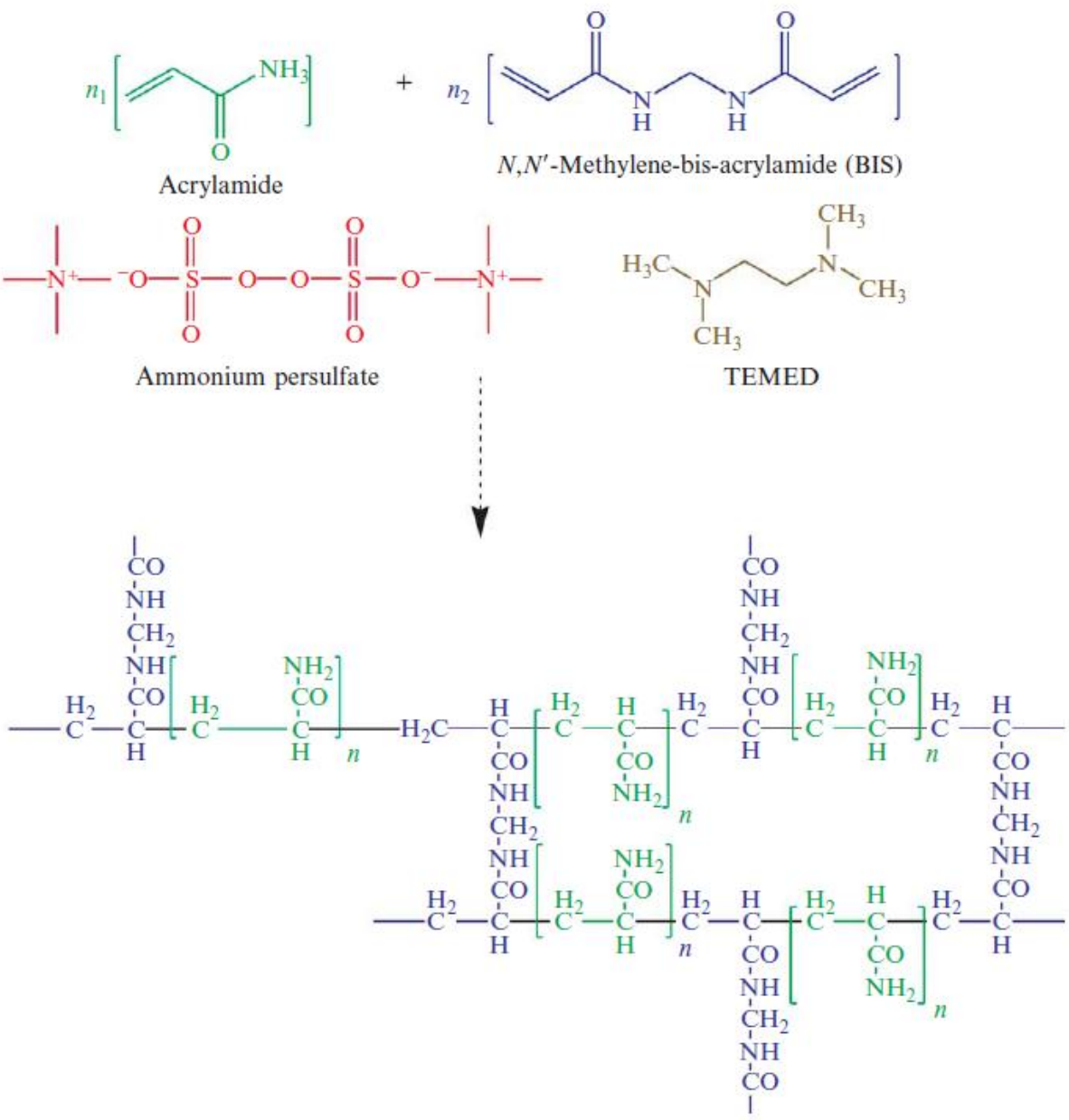

Figure 2.3. PA gel formation from acrylamide monomers and bis-acrylamide crosslinkers. Ammonium persulfate generates free oxygen radicals in the presence of TEMED, a catalyst (Kandow, Georges et al. 2007).

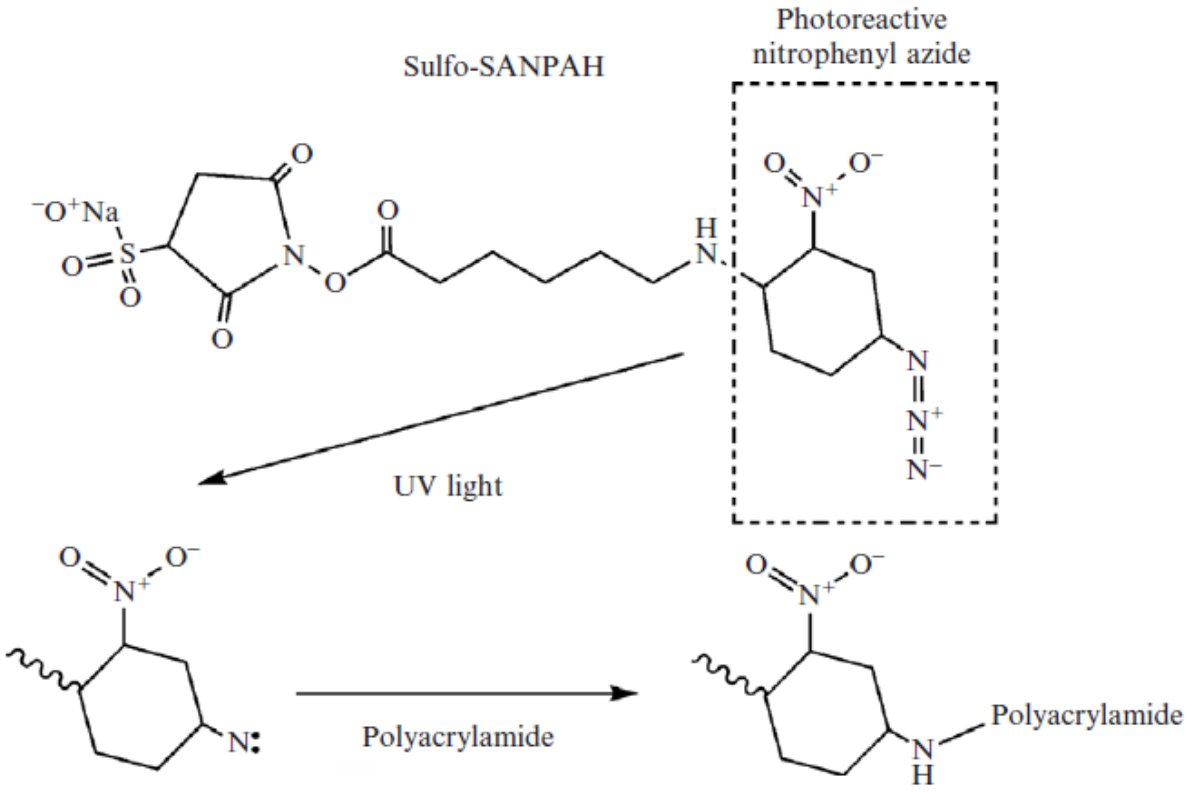

Figure 2.4. Sulfo-SANPAH, a heterobifunctional photoractive reagent becomes photoactivated when the phenylazide reactive group is exposed to UV. It then forms a nitrene group that reacts nonspecifically with PA. The sulfosuccinimydyl group at the other end reacts with primary amine groups of the protein of choice (Kandow, Georges et al. 2007).

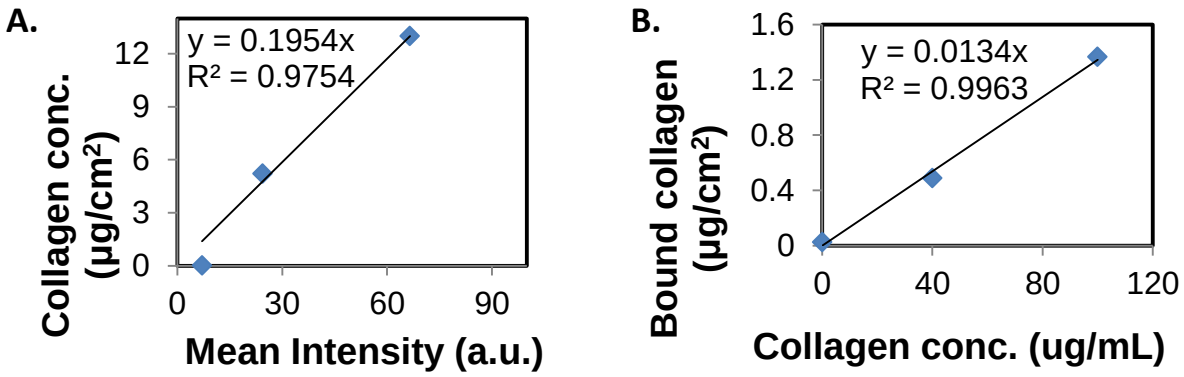

Figure 2.5. Calibration curves for determining the amount of surface-bound collagen. 200 µL of 1 ng/mL – 100 µg/mL collagen solutions were deposited to serve as standards (A).

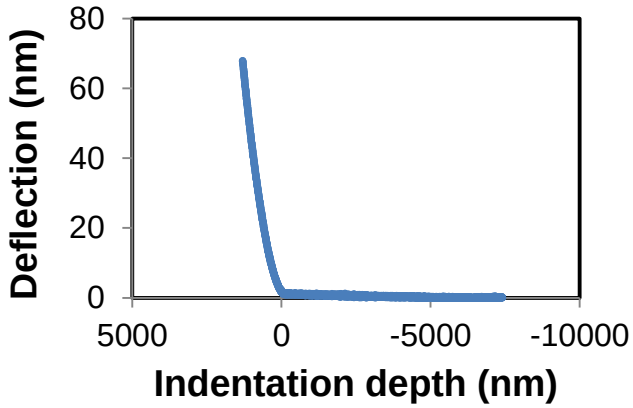

Figure 2.6. Force-indentation curve (extraction only) for 8.75 kPa PA gel. The slope of the curve correlates with the stiffness of the sample. Stiffer samples have steeper curves.

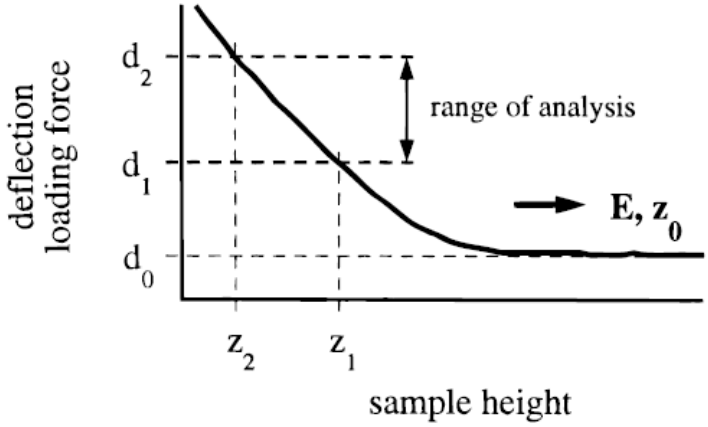

Figure 2.7. Force-indentation curve with the zero deflection (force) d_0 and the range of analysis defined by two data points (d_1, z_1) and (d_2, z_2). Analysis on this data yields the contact point z_0 and the Young's modulus E (Domke and Radmacher 1998).

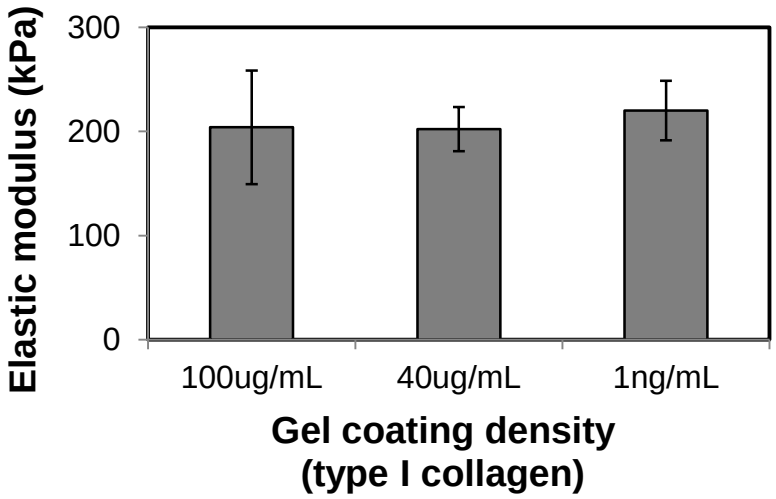

Figure 2.8. PA gels (38% acryl/ 2% bis-acryl) were coated with three different coating densities (100 μg/mL, 40 μg/mL, or 1 ng/mL) and probed with AFM to measure their elastic moduli (shown with standard deviations). The PA gel coating density did not significantly affect the stiffness of the gels.

2.6. Tables

Collagen concentration	Elastic Modulus (Pa)
1.45 mg/mL	14.8 ± 6.1
2.9 mg/mL	44.2 ± 10.7

Table 2.1. Elastic moduli of collagen hydrogels were determined via Rheology. Both collagen hydrogels (1.45 and 2.9 mg/mL) are very soft with $E < 1$ kPa.

	Literature†	Uncoated
%Acryl/%Bis-acrylamide (v/v)	**Young's Modulus (kPa)**	**Young's Modulus (kPa)**
4/0.03	0.71 ± 0.24	-
5/0.10	3.15 ± 0.85	3.48 ± 0.59
5/0.26	8.58*	8.75 ± 1.21
38/2	-	196 ± 54.1

* Extrapolated with reported moduli
† (Tse and Engler 2010)

Table 2.2. Elastic moduli of PA hydrogels were computed from AFM force measurement data and compared to previously reported values in the literature

CHAPTER 3: HSC CULTURE AND OBSERVED BIOPHYSICAL CHANGES

3.1. Introduction

HSCs were harvested from the femurs and tibias of C57B6 mice and were cultured on top of or inside collagen hydrogels or on top of 2D PA gels with varying mechanical properties for 24 hours then analyzed. Changes observed in HSCs at the end of the 24-h culture are summarized in this chapter.

3.2. Isolation of HSCs

HSCs were isolated from the femurs and tibias of 4 – 10-week-old female C47Bl\6 mice (The Jackson Laboratory, Bar Harbor, ME) via fluorescence activated cell sorting (FACS). Briefly, mice were euthanized with carbon dioxide in compliance with the University of Illinois Institutional Animal Care and Use Committee (IACUC) guidelines. Their femurs and tibias were then collected, crushed, and filtered through a 40-μm cell strainer (BD Falcon, Franklin Lakes, NJ) to yield a whole bone marrow cell suspension in PBS supplemented with 2% FBS. Red blood cells were removed by incubating the cell suspension in ACK lysing buffer (Invitrogen, Carlsbad, CA) for 15 minutes. Nonspecific binding was inhibited by incubating the cell suspension with Fc receptor block (CD16/CD32) for 15 minutes. Cells were then labeled by incubating in a cocktail of antibodies consisting of FITC-conjugated lineage (Lin) antibodies (CD5, CD45R (B220), CD11b, Anti-Gr-1 (Ly-6G/C), 7-4, Ter-119), PE-conjugated Sca-1, and APC-conjugated c-Kit. (All antibodies were purchased from eBiosciences, San Diego, CA). Labeled cell suspension was filtered into a polystyrene round-bottom tube with a 40-μm cell

strainer cap to remove any cell clumps. All steps were performed at 4 ℃ and cells were centrifuged at 1400 rpm for 5 minutes and re-suspended in PBS with 2% FBS between steps. Labeled were cells were sorted using BD FACSAria™ cell sorter (BD Biosciences, San Jose, CA) for $Lin^{-}Sca\text{-}1^{+}c\text{-}Kit^{+}$ cells. Dead cells were excluded with propidium iodide (PI) staining. A detailed protocol showing HSC harvest procedures can be found in **Appendix B.1.**

3.3. HSC culture conditions

LSK population ($Lin^{-}Sca\text{-}1^{+}c\text{-}Kit^{+}$) harvested from mouse BM were seeded at a cell seeding density of 7,000 – 8,000 cells/sample on 2D PA gels coated with type I collagen (100 µg/mL) or on top of collagen hydrogels. Alternatively, a cell suspension containing 7,000 – 8,000 cells was mixed with type I collagen, culture medium, 1M HEPES, and 0.4M NaOH right before the start of culture to create a 3D collagen hydrogel construct. HSC culture medium was prepared according to a published method with a slight modification (Lutolf, Doyonnas et al. 2009): a serum-free Stemline® II hematopoietic stem cell expansion medium (Sigma, St. Louis, MO) was supplemented with 100 ng/mL SCF (Stem Cell Technologies, Vancouver, Canada) and 4 ng/mL Flt-3/Flk-2 ligand (Stem Cell Technologies Vancouver, Canada). HSCs were incubated in a humidified incubator at 37℃ with 95% oxygen and 5% CO_2 supply for 24 hours.

As a control group, bareglass collagen-coated glass substrates were utilized. Both bareglass bottom dishes and collagen-coated glass substrates were purchased from MatTek Corp., Ashland, MA.

3.4. HSC viability

After 24 hours of culture, cells were incubated in LIVE/DEAD Cell Viability Assay (Invitrogen, Carlsbad, CA). Stained cells were imaged with Leica DMI4000 inverted microscope with a 40x objective at five different spots. The numbers of live (calcein, green) versus dead (ethidium homodimer-1, red) cells at these spots were scored and averaged to obtain the mean cell viability of the corresponding sample. Protocol for performing viability assay is presented in **Appendix B.2.**

Figure 3.2. compares the viability of HSCs cultured on substrates with varying stiffness. HSCs showed increased viability on 2.9 mg/mL collagen hydrogels with an elastic modulus of 0.0442 kPa. Cell viability was lowest on uncoated glass samples, which suggests that cell attachment to the substrate through ligand-receptor interactions is important in maintaining HSC viability. HSCs showed slightly increased viability when cultured on stiffer 2D PA gels.

3.5. Biophysical changes observed in HSCs

At the end of the 24-hour culture, HSCs cultured inside or on top of 3D collagen hydrogel structures and on top of 2D PA gels were fixed with 3.7% paraformaldehyde and stained to visualize their actin structures. A detained staining protocol can be found in **Appendix B.3.** Stained samples were imaged with a multiphoton laser scanning microscope (LSM 710; Carl Zeiss AG, Thornwood, NY) with a 63x objective (numerical aperture = 1.4) in order to create 3D confocal images of the cells attached to the substrates. Zen software (Carl Zeiss AG, Thornwood, NY) was used for image acquisition.

3.5.1. Effects of dimensionality (2D vs. 3D) on HSCs

HSCs were seeded on top of 3D collagen hydrogels to provide 2D-like culture conditions or encapsulated in the same hydrogel constructs for a 3D culture environment. The effects of dimensionality, although subtle, were observed in terms of cell viability and the level of cytoskeletal organization. As shown in **Figure 3.3.**, HSCs cultured inside 3D collagen hydrogel constructs showed decreased cell viability compared to those cultured on top of 3D collagen hydrogels with the same stiffness. This pattern was observed for both 1.45 and 2.9 mg/mL collagen hydrogels.

Figure 3.4. shows morphological differences in HSCs cultured on top of collagen hydrogels or inside collagen hydrogel constructs. Firstly, HSCs cultured on top of or inside stiffer collagen hydrogels (2.9 mg/mL; 0.0442 ± 0.0107 Pa) showed more cytoskeletal development or cytoplasmic protrusions compared to those grown on top of or inside softer collagen hydrogels (1.45 mg/mL; 0.0148 ± 0.0061 Pa). Secondly, HSCs cultured on top of 3D collagen hydrogels (‘2D’-like) were more spread out compared to those that were encapsulated in 3D constructs, which retained more rounded morphology. In stiffer 3D constructs (2.9 mg/mL), HSPCs started developing thin, filopodial protrusions forming at the cytoplasmic region enriched in F-actin fibers, although they still maintained overall more rounded morphology compared to those grown on top of the ‘2D’ equivalents.

3.5.2. Effects of substrate elasticity on HSCs

The spread area and cell shape index (CSI) of the HSCs cultured on top of '2D' substrates were calculated via ImageJ from projected 2D images of the cells gathered with confocal microscopy. Briefly, the images were thresholded and cells defined by the distribution of actin fibers were outlined in order to compute the spread area and the perimeter of the cells. CSI, which is a measure of the circularity of a cell, is a dimensionless ratio given by:

$$\mathrm{CSI} = \frac{4\pi(cell\ area)}{(cell\ perimeter)^2} \qquad \textbf{(Equation 3.1.)}$$

has values between 0 and 1. CSI approaches 0 as the cell morphology deviates from being a perfect circle (Thakar, Chown et al. 2008). For all image analyses, single cells not in direct contact with one another were analyzed. Dividing cells were also excluded. **Appendix B.4.** includes a detailed protocol for cell image manipulation using Image J for cell spread area calculations.

Significant differences were noted in the spread area of HSCs cultured on substrates with varying elasticity (**Figure 3.5.**). On top of soft collagen hydrogels with stiffness lower than about 2 kPa, reminiscent of the stiffness of the marrow and adipose tissue, HSCs spread out more than on the gels resembling the stiffness of a single cell, which is in the 1-100 kPa stiffness range (Radmacher 1997), with many cell types exhibiting low kPa Young's moduli. On really stiff gels, cells spread out significantly more. However, when ligand was not present as in bareglass substrates, cells spread out only as much as they did on soft gel samples, suggesting the potentially importantly role played by substrate ligand density.

HSCs are small, circular cells with a diameter of only about 5 µm when they are first harvested from a mouse. Within 24 h of culture, they spread out considerably with increasing substrate elasticity but maintained relatively circular cell shape throughout, with just a slight decrease in cell circularity with increasing substrate stiffness (**Figure 3.6.**). Cells on uncoated glass slides remained more circular compared to those cultured on collagen-coated glass slides.

3.5.3. Effects of substrate ligand density on HSC morphology

To verify the importance of substrate ligand concentration in dictating HSC biophysical behavior, three different collagen coating densities (100 ug/mL, 40 ug/mL, 1 ng/mL) were applied to the 196 kPa PA gels. The results showed a significant decrease in both cell viability and cell spread area with decreasing ligand coating density (**Figure 3.7. (a)** and **(b)**). Moreover, decreasing collagen-coating density was correlated with increased CSI values, which means that cells retained more circular morphology as the ligand concentration was dropped (**Figure 3.7.(c)**).

3.5.4. Effect of substrate stiffness on HSC cytoskeletal density distribution

In 2009, Chowdhury *et al.* found that applying a local cyclic force on embryonic stem cells (ESCs) induced cell spreading and downregulation of oct3/4 gene via focal adhesion-dependent mechanisms. This phenomenon was not seen in further differentiated cells (i.e., mouse embryonic stem-cell-differentiated cells) which were roughly ten times stiffer than ESCs, suggesting that the spreading responses were based on the cell material property (cell softness). F-actin was identified to be one of the essential mediators of the spreading response as F-actin

densities were inversely related to cell softness (Chowdhury, Na et al. 2009). Cell deformability study via micropipette aspiration also proposed that cell softness may be a function of the differentiated state (i.e. stemness) of the cell (Pajerowski, Dahl et al. 2007). Thus, it seemed appropriate to elucidate the role of F-actin distribution on HSCs cultured on different substrates to monitor their status in relation to the changes made to their biophysical properties.

In order to verify the role of F-actin distribution on HSCs, F-actin densities were examined in a way similar to previously reported (Chowdhury, Na et al. 2009). Briefly, F-actin expression along three different cross-sectional regions of a cell was quantified for HSCs cultured on 2D PA substrates with varying stiffness. Fluorescence intensity of F-actin over each cross-section revealed regions of dense actin fibers near the cell edge, evident from the peak formed at the cortex (**Figure 3.8.(A)**). In order to eliminate the differences in fluorescence intensity arising from different laser settings, the peak was normalized with respect to the relative cell length (x) and baseline intensity (y) (**Figure 3.8.(B)**). HSCs cultured on 2D PA substrates showed increasing y as substrate stiffness increased (**Figure 3.8.(A)**), where increasing y correlated with increasing F-actin density. However, the differences were masked largely by the internal normalization of the fluorescence intensity.

3.6. Discussion

3.6.1. Substrate mechanics on HSC fate

While Holst *et al* (Holst, Watson et al. 2010) recently suggested that substrate tensegrity provides mechanical signals regulating HSPC expansion, studies on HSC biology through HSC-

niche interactions have been largely limited to *in vivo* experiments with knockout or transgenic mice, and surprisingly little effort has been put in to decouple the effects of mechanics of the physical environment where HSCs reside.

In vivo, HSCs are exposed to soft tissues such as adipose tissue with a Young's modulus of only < 2 kPa (Discher, Mooney et al. 2009) up to collagenous bone with a stiffness of 25 – 40 kPa (Engler, Sen et al. 2006). 2D PA gels and 3D collagen hydrogels culture system with tunable mechanical properties, matrix elasticity could be further decoupled from other factors (growth factors, cell-cell interactions, etc.) in probing HSC fate.

HSPC viability, spread area, and cell shape data give insight on how HSCs might behave in a microenvironment rich in certain components (i.e., fat-rich environment (< 2 kPa), other cell types (~3 kPa), hard tissues such as bone (~100 kPa)). HSPC viability was enhanced at 0.0442 kPa (**Figure 3.2.**), which suggests that HSCs may survive better on softer substrates. *In vivo*, this may refer to being in the vascular niche (rich in marrow) versus in the endosteal niche (at the bone interface). However, HSC viability was low in general due to poorly characterized *in vitro* HSC culture conditions. Currently, no well-established protocols exist for maintaining HSCs viable in culture for a long period of time. Further studies on HSC-matrix interactions utilizing immobilized growth factors or additional cytokines (IL-3, TPO, etc.) will be useful in finding optimal HSC culture conditions.

HSC spread area increased significantly with increasing substrate elasticity (**Figure 3.5.**). When cultured on stiff substrates (196 kPa), HSCs spread out approximately twice as much as they did

on substrates with an effective single cell stiffness (3.48 kPa; $p < 0.5$). HPSCs spread out even more on collagen-coated glass substrates (E_{glass} = ~70 GPa; $p < 0.001$; (Schneider, Francius et al. 2005)), but significantly less on uncoated glass substrates. This suggests that receptor-ligand interactions as well as substrate elasticity modulate HSC spreading. Overall, HSCs retained rounded morphology as the cell shape index remained at ~0.6 or greater on all substrates (**Figure 3.6.**). However, HSCs became slightly more amorphous with higher degrees of membrane ruffling as substrate stiffness increased. Again, HSCs cultured on uncoated glass substrates maintained more circular morphology compared to those cultured on collagen-coated glass substrates.

To further quantify receptor-ligand interactions on HSC behavior, HSCs were cultured on stiff PA substrates (196 kPa) coated with three different collagen coating concentrations (100 μg/mL, 40 μg/mL, 1 ng/mL). Viability was significantly impacted, with almost no HSCs surviving at 1 ng/mL collagen-coating. HSC spread area also decreased and they remained more rounded with decreasing collagen coating density (**Figure 3.7.**). These results imply that HSC binding through ECM proteins such as type I collagen is important in regulating HSC fate. In future experiments, HSC interactions with other ECM proteins (fibronectin, laminin, vitronectin) could also be explored to further characterize HSC-ECM interactions.

Substrate stiffness also affected cytoskeletal density, measured by F-actin fluorescence intensity. Although changes were masked by internal normalization, there was denser actin organization in the leading edge of HSCs cultured on stiffer substrates (**Figure 3.8.**). These differences suggest

that the stiffness of HSCs themselves may vary with substrate stiffness, although actin fibers were punctate and did not form stress fibers within 24 hours of culture.

3.6.2. 2D vs. 3D culture system

2D PA gels allow substrate elasticity to be decoupled and tested independently. However, they do not fully reconstitute *in vivo* microenvironments where cells are presented with 3D living conditions. To probe the effect of dimensionality on cells, soft collagen hydrogels were utilized. Cells were plated on top of these collagen hydrogels or were encapsulated in collagen hydrogel constructs. This system, however, was limited to low modulus settings (< ~0.5 kPa).

The effect of dimensionality can be observed from the images of HSCs (**Figure 3.4.**). Qualitatively, HSCs retained more rounded morphology in 3D collagen constructs. Gene expression assays or other functional assays to assess the stemness of HSPCs cultured on top of or inside hydrogels with the same mechanics would be an interesting addition of data that would quantify the effect of dimensionality on HSC functionality.

3.7. Figures

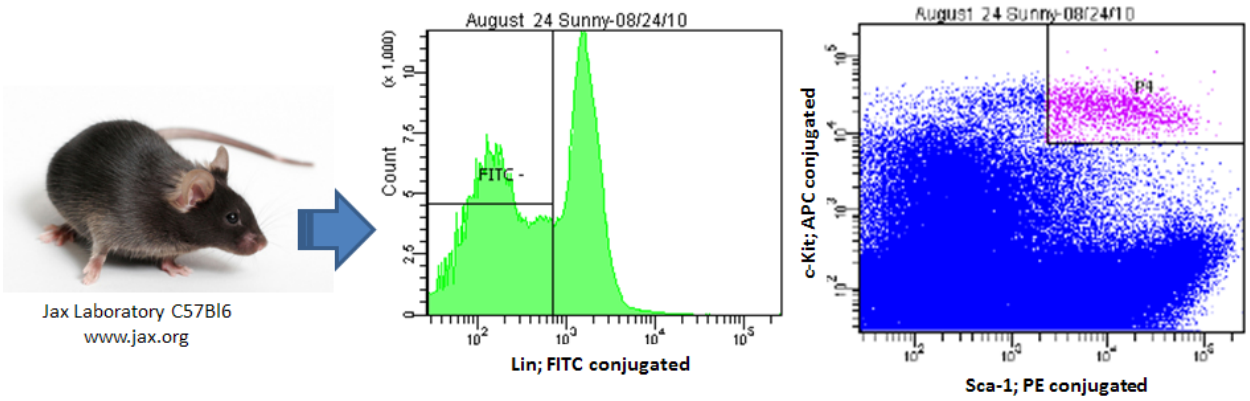

Figure 3.1. HSCs are harvested from femurs and tibias of C57B6 mouse. Identification and collection of LSK ($Lin^{-}Sca\text{-}1^{+}c\text{-}Kit^{+}$)population is shown.

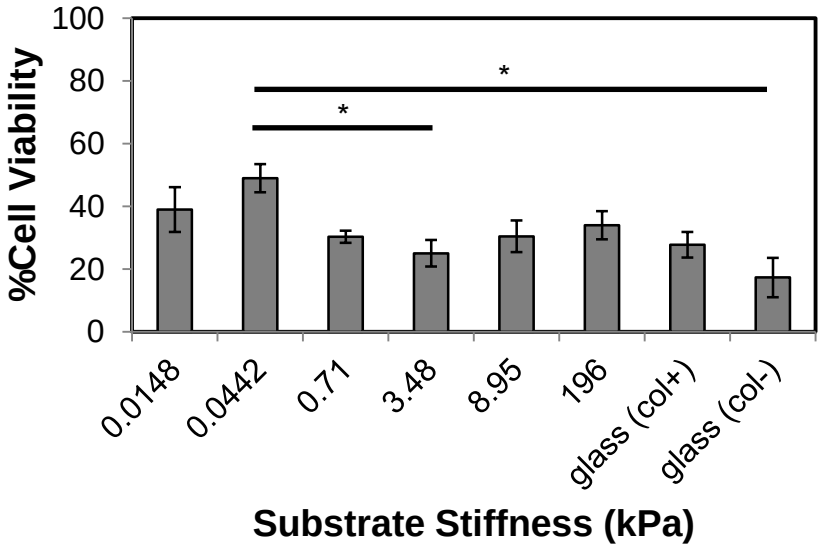

Figure 3.2. % Viability of HSCs cultured on substrates with varying stiffness for 24 hours. First two columns (0.0148 and 0.0442 kPa) refer to collagen hydrogels. The next four data groups correspond to PA gel substrates.

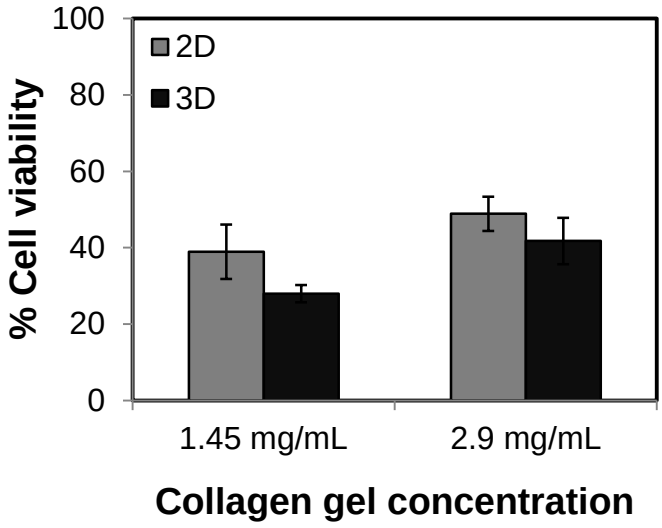

Figure 3.3. Viability (%) of HSCs cultured on top of or inside 3D collagen hydrogels for 24 hours.

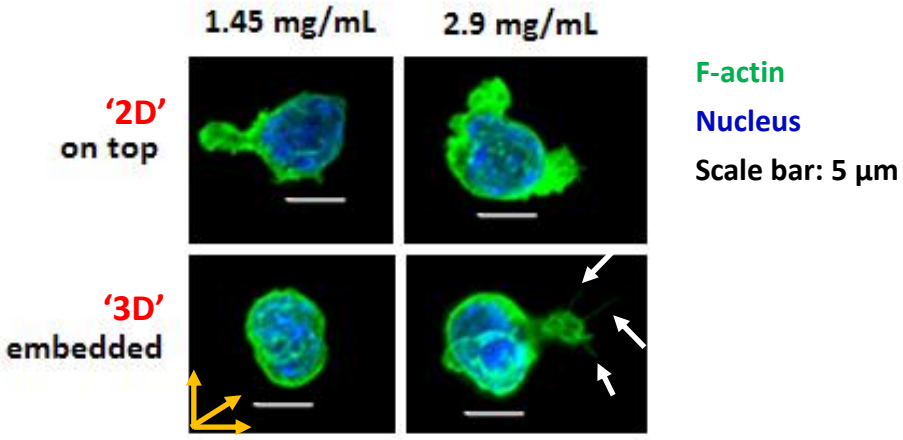

Figure 3.4. HSCs cultured on top of or inside collagen hydrogels for 24 hours were fixed and stained to visualize morphology and the actin skeletal organization. Images are 2D projected images of the 3D stacked images obtained via confocal fluorescence microscopy. Scale bar: 5 µm.

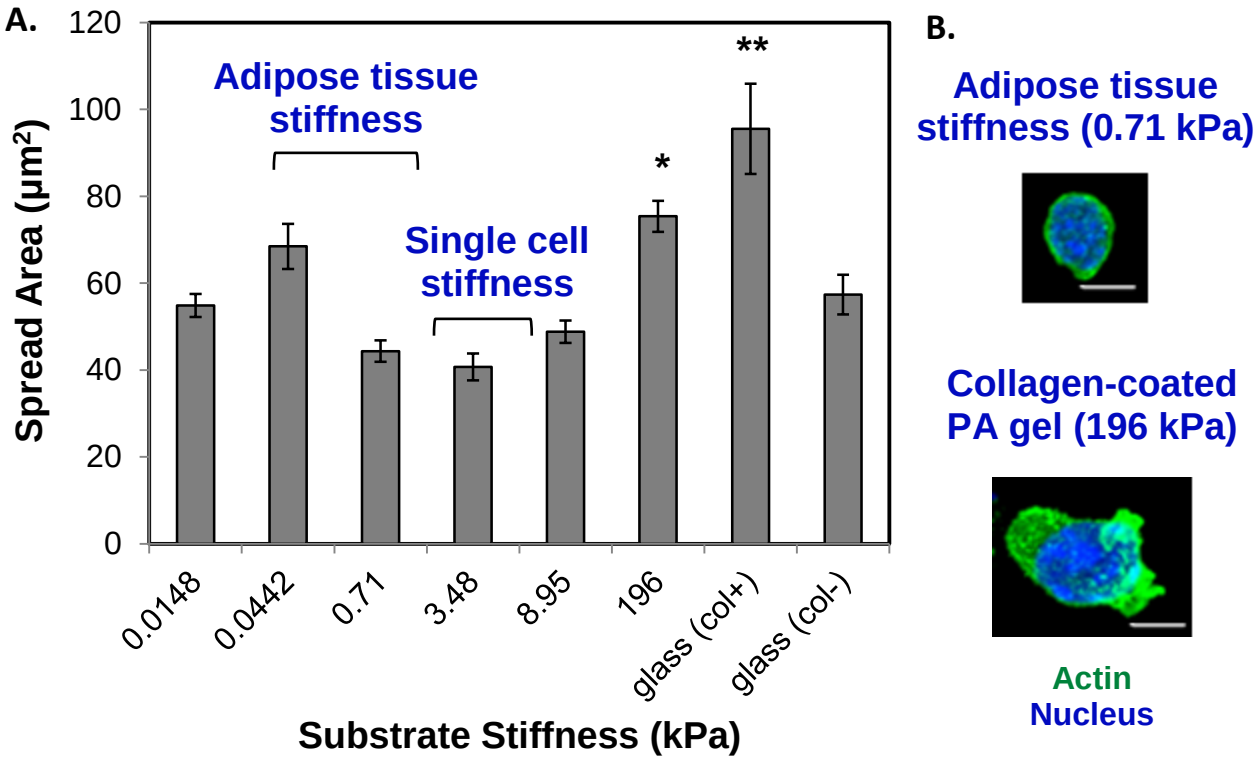

Figure 3.5. Spread area after 24-h culture. HSCs were cultured on top of collagen hydrogels and 2D PA substrates for 24 hours then fixed and stained. They were then imaged to calculate their spread area (A). Representative fluorescence images of HSCs cultured on PA gels with different Elastic moduli are shown in (B).

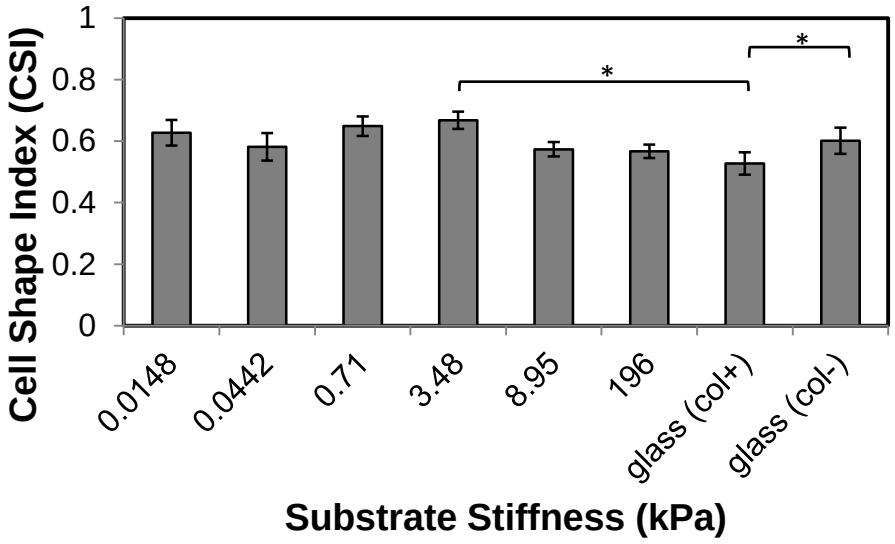

Figure 3.6. CSI after 24-h culture. HSCs were cultured on top of collagen hydrogels and 2D PA substrates for 24 hours then fixed and stained. They were then imaged to calculate their CSI.

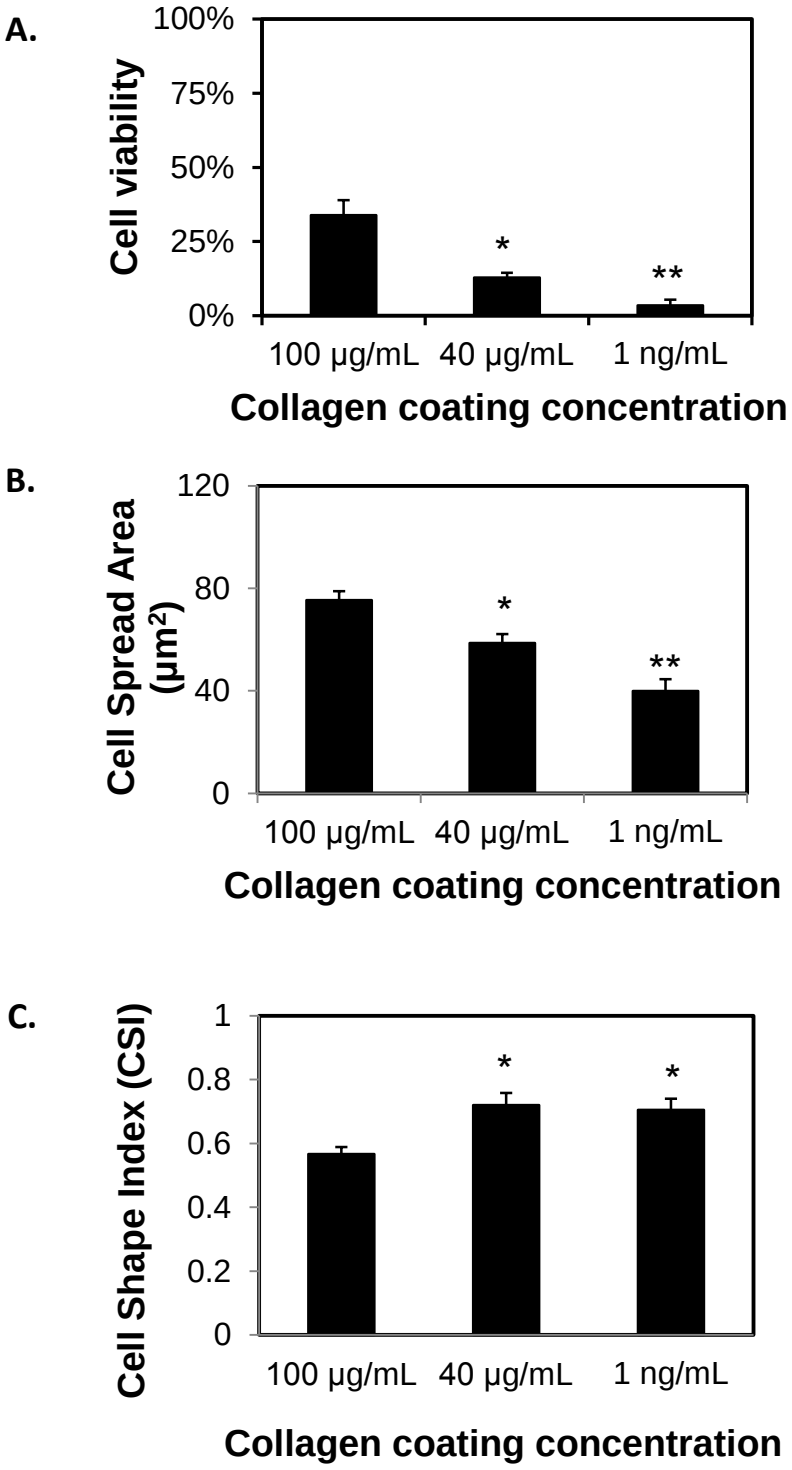

Figure 3.7. % cell viability (A), cell spread area (B), and CSI (C) for HSCs cultured on 196 kPa PA gels coated with three different collagen densities (100 µg/mL, 40 µg/mL, 1 ng/mL) for 24 hours.

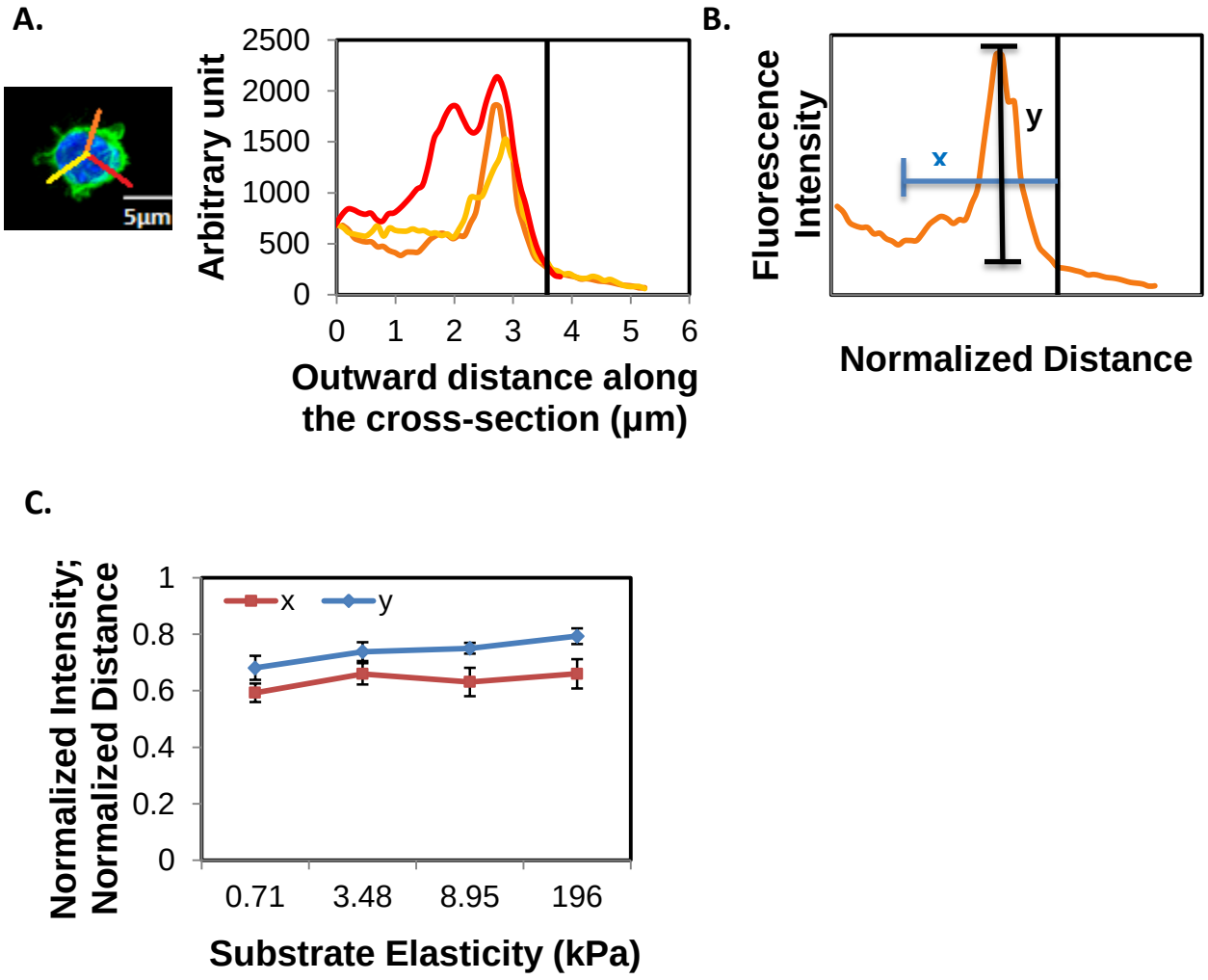

Figure 3.8. Fluorescence intensity of F-actin over each cross-section revealed regions of dense actin fibers near the cell edge, evident from the peak formed at the cortex (A); Peak normalization with respect to the relative cell length (x) and baseline intensity (y) (B); CSK distribution (C).

3.8. Conclusions

While Holst *et al* (Holst, Watson et al. 2010) recently suggested that substrate tensegrity provides mechanical signals regulating HSPC expansion, studies on HSC biology through HSC-niche interactions have been largely limited to *in vivo* experiments with knockout or transgenic mice, and surprisingly little effort has been put in to decouple the effects of mechanics of the physical environment where HSCs reside.

In vivo, HSCs are exposed to soft tissues such as adipose tissue with a Young's modulus of only < 2 kPa (Discher, Mooney et al. 2009) up to collagenous bone with a stiffness of 25 – 40 kPa (Engler, Sen et al. 2006). 2D PA gels and 3D collagen hydrogels culture system with tunable mechanical properties (matrix elasticity, matrix ligand presentation) were used to decouple variables in probing HSC fate. Significant differences in HSC viability and morphology were observed with varying substrate elasticity.

CHAPTER 4: 32D CELL CULTURE AND OBSERVED BIOPHYSICAL CHANGES

4.1. Introduction

In order to compare HSC behavior with a more committed cell population, 32D cells were used as a control. They were cultured using the same collagen hydrogels and PA gels used to culture HSCs and analyzed.

4.2. 32D cell line

32D cells are interleukin-3 (IL-3) dependent murine myeloid progenitor cells that are widely used as an *in vitro* model of hematopoiesis to study hematopoietic cell behaviors including proliferation, differentiation, and apoptosis. They terminally differentiate into neutrophilic granulocytes upon the removal of IL-3 and injection of granulocyte-colony stimulating factor (G-CSF) to the culture medium, and this differentiation process closely resembles the differentiation patterns inside the marrow (Valtieri, Tweardy et al. 1987; Agliano, Santangelo et al. 2000).

4.3. 32D cell culture conditions

The 32D clone 3 (32D Cl3) or CRL-11346 cell line was purchased from ATCC (Manassas, VA,). Purchased 32D cells were thawed and subcultured according to ATCC protocols in a complete growth medium prepared by supplementing RPMI 1640 medium, which was modified to contain 10 mM HEPES, with 1 mM sodium pyruvate, 4.5 g/L glucose, 1.5 g/L sodium

bicarbonate, and 2 mM L-glutamine, 10% heat inactivated FBS and 10% mouse IL-3 culture supplement (BD Sciences, Franklin Lakes, NJ).

Similar to HSCs, 32D cells were seeded at 7,000 – 8,000 seeding density on top of 2D PA gels and 3D collagen hydrogels ('2D'). Alternatively, a cell suspension containing 7,000 – 8,000 cells was mixed with type I collagen, culture medium, 1M HEPES, and 0.4M NaOH at the start of culture to create 3D collagen hydrogel constructs. The cells were incubated in a humidified incubator at 37℃ with 95% oxygen and 5% CO_2 supply for 24 hours.

4.4. 32D cell viability

Regardless of the substrate stiffness or substrate ligand density with which the 32D cells were grown, they showed % cell viability of roughly 80% or higher (data not shown). This is expected because 32D cells are from a well-established cell line.

4.5. Biophysical changes observed in 32D cells

As mentioned in previous sections, 32D cells are murine IL-3 dependent myeloid progenitor cells from a cell line. 32D cells are not anchorage-dependent cells and the vast majority stays as small, rounded cells in suspension when cultured for expansion.

4.5.1. Effects of dimensionality (2D vs. 3D) on 32D cells

Similar to HSCs, 32D cells grown either on top of ('2D') or inside ('3D') collagen hydrogels were fixed, stained, and imaged (**Figure 4.1.**). 32D cells were overall about three times bigger compared to HSCs cultured for 24h. Also because these cells were from a cell line, their viability was 80% or greater. 32D cells in 3D constructs were able to develop large cytoplasmic regions growing outward within 24-h of culture, and these were larger in stiffer (2.9 mg/mL) constructs. Also, the nuclei of 32D cells in 3D constructs tended to be bent in the direction of the cytoplasmic protrusions because they could not freely spread out in the x-y plane like those cultured on top of collagen hydrogels.

4.5.2. Effects of substrate elasticity on 32D cells

32D cells showed a similar trend in cell spreading area with HSCs, with a peak in spread area at a low stiffness substrate (0.0442 kPa) and increasing spread area with increasing PA gel stiffness, although the increase was subtle. Interestingly, 32D cells were able to spread out considerably on bareglass even without the collagen-coating.

32D cells developed more cytoskeletal protrusions around the cell edges, and these deviations from the cell circularity were reflected in significantly decreased CSI values at increased substrate stiffness greater than 0.71 kPa (**Figure 4.3.**).

4.5.3. Effects of substrate ligand density on 32D cells

There was significant spreading and cytoskeletal organization for the 32D cells cultured on bareglass without any collagen coating, probably because 32D cells overall can attach to

substrates more strongly to spread out much more compared to HSCs. These results suggested that these might behave differently from HSCs with varying substrate ligand density, and that is what was observed when 32D cells were cultured on 196 kPa PA gel substrates with three different collagen-coating densities: 100 ug/mL, 40 ug/mL, 1 ng/mL. Cell spread area was optimal at an intermediate collagen coating density (40 ug/mL). Cell morphology was also deviating most from being a perfect circle at this concentration, as can be seen in **Figure 4.4.** Previous studies with smooth muscle cells exhibited similar cell spreading behaviors, where cell spreading was optimal at an intermediate collagen density (Engler, Bacakova et al. 2004).

4.6. Discussion

32D cells are a hematopoietic progenitor cell line (Bersenev, Wu et al. 2008) that is often used to study HSPC behavior *in vitro*. 32D cells can stay undifferentiated indefinitely as long as they are cultured with an IL-3 containing medium. Upon removal of IL-3 and introduction of G-CSF, they terminally differentiate to become granulocytes (Agliano, Santangelo et al. 2000). 32D cells behaved very differently from HSCs when they were cultured on the same set of collagen hydrogels and PA gels. Overall, they showed highly amorphous morphology with CSI below 0.4 on substrates with a stiffness greater than 0.71 kPa (**Figure 4.3.**) as well as being approximately twice as large as HSPCs after 24 h of culture. Their spread area tended to increase with an increasing substrate stiffness (**Figure 4.2.**), but they showed different biophysical patterns when different ligand concentrations were presented (**Figure 4.4.**). Their viability was not affected by decreasing collagen-coating concentration (data not shown) and they spread out most on an intermediate collagen coating (40 μg/mL). CSI was also lowest at this concentration. These

results confirm that 32D cells are further differentiated downstream cells that are governed by different mechanisms.

4.7. Figures

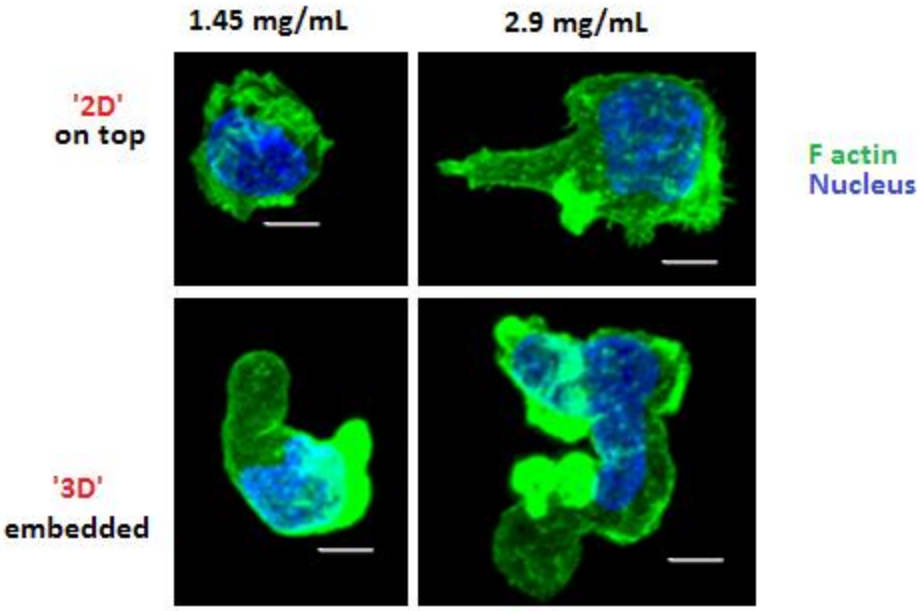

Figure 4.1. 32D cells cultured on top of ('2D') or inside ('3D') collagen hydrogels for 24 hours were fixed and stained to visualize morphology and the actin skeletal organization. 2D projected images of the 3D stacked images of the cells are obtained via confocal fluorescence microscopy. Scale bar: 5 µm.

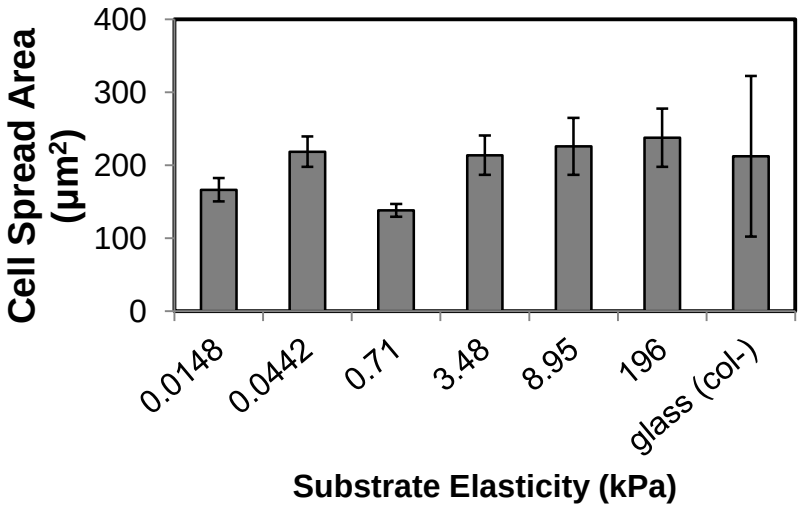

Figure 4.2. Spread area after 24-h culture. 32D cells were cultured on top of collagen hydrogels and 2D PA substrates for 24 hours then fixed and stained. They were then imaged to calculate their spread area. For cell image analysis protocol, refer to **Appendix B.4.**

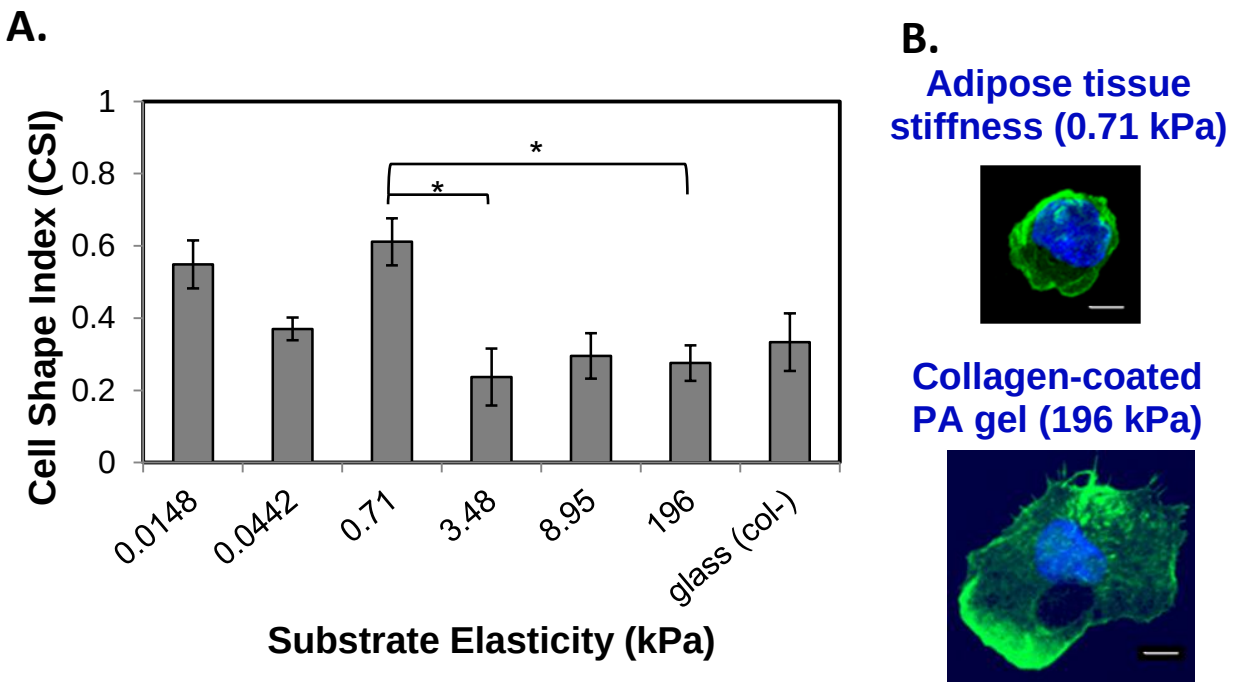

Figure 4.3. CSI after 24-h culture. 32D cells were cultured on top of collagen hydrogels and 2D PA substrates for 24 hours then fixed, stained, and imaged to calculate CSI.

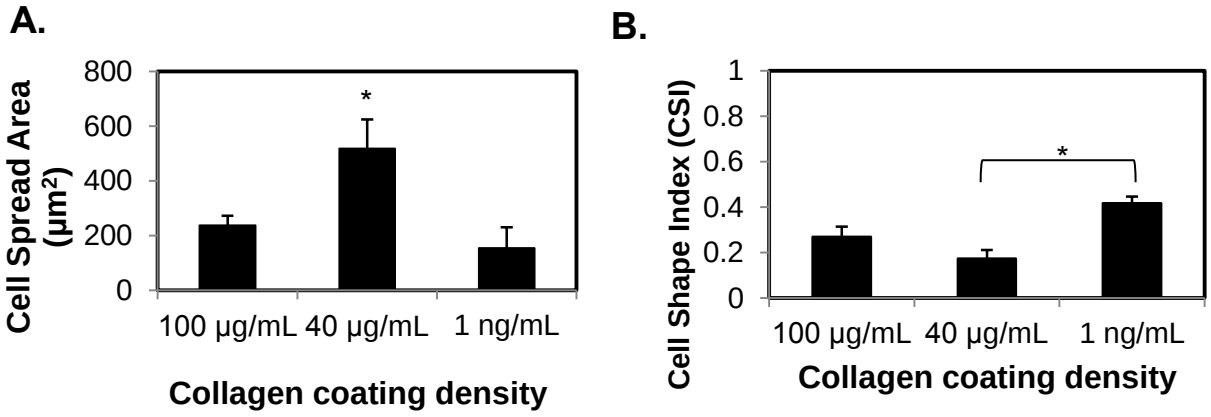

Figure 4.4. Spread area (a) and CSI (b) changes with varying substrate ligand density. 32D cells spread out most at an intermediate ligand density of 40 μg/mL.

4.8. Conclusions

32D cells showed similar patterns in spreading (spread area) but different patterns in cell morphology (CSI) with varying substrate elasticity and substrate ligand density as compared to HSCs when they were cultured on top of or inside collagen hydrogels and on top of PA gels for 24 hours.

CHAPTER 5: CONCLUSIONS

5.1. Conclusions

Collagen hydrogels and PA gels were fabricated and mechanically characterized via rheology and AFM to give substrate stiffness ranging from < 1 kPa to ~200 kPa. HSCs harvested from C57B6 mouse femurs and tibias and 32D cells, IL-3 dependent murine myeloid progenitor cells (cell line) were cultured either on top of or inside collagen hydrogels or on top of collagen-coated PA gel substrates. Changes in viability, spread area, morphology, and cytoskeletal reorganization were observed in cultured cells. Substantial differences between HSCs and 32D cells were also discovered, especially regarding substrate ligand presentation and ligand density.

By further elucidating the effects of substrate elasticity (especially physiologically relevant range of stiffness) and combining the results with those gathered from cell-cell or cell-growth factor interaction studies, it will eventually be possible not only to gain a better understanding of the HSC regulation mechanisms but recreate the HSC niches *in vitro* for precise control of HSC fate for various clinical applications.

5.2. Future work

The next objective to be completed is to check the functionality of cultured HSCs using methylcellulose-based colony forming cell (CFC) assays. This assay allows the detection of the presence of primitive HSCs and/or more committed progenitors by counting the number of CFCs formed at day 10-12 of culture. It is an alternative to validating functionality of HSPCs with lethally irradiated mouse models.

HSC-ECM interactions will further be analyzed by using other ECM proteins (fibronectin, laminin, and vitronectin). A gradient PA gel with varying stiffness and a gradient of immobilized surface protein is also being investigated and considered for future studies of cell-ECM interactions and chemokine-induced cell migration studies.

Similar to what Holst *et al.* showed, whole murine BM cell cultures will also be analyzed for HSC expansion and differentiation. After these studies are performed and analyzed, gene expression of the cultured cells will also be carried out to monitor any up- or down-regulation of stem-cell specific genes.

APPENDIX A: GEL FABRICATION AND CHARACTERIZATION PROTOCOLS

A.1. Collagen hydrogel fabrication protocol

REFERENCES: (Baker, Bonnecaze et al. 2009; Yang and Kaufman 2009)

SUPPLIES

Type I collagen from rat tail (BD Biosciences, Bedford, MA); Respective cell culture medium; 1M HEPES buffer; 0.4 M NaOH; 10-mm or 14-mm glass bottom dish (MatTek Corp., Ashland, MA)

EQUIPMENT

Biological safety cabinet; pH meter; 37 ℃ incubator

PROCEDURE

NOTE: Pre-cool all reagents required for collagen gel fabrication to 4 ℃ before use to prevent any premature collagen gelation upon mixing.

1. Dilute collagen stock solution (8.25 mg/mL to 9.33 mg/mL) with the respective cell culture medium to bring the final concentration to 1.45 or 2.9 mg/mL, as desired. Make 1-mL or 2-mL working volume of the collagen mixture.

2. Add 50 µL of 1 M HEPES buffer and appropriate amounts of 0.4 M NaOH to bring the pH to 7.4 according to previously established calibration curves. An example of such curve is shown below. Mix well.

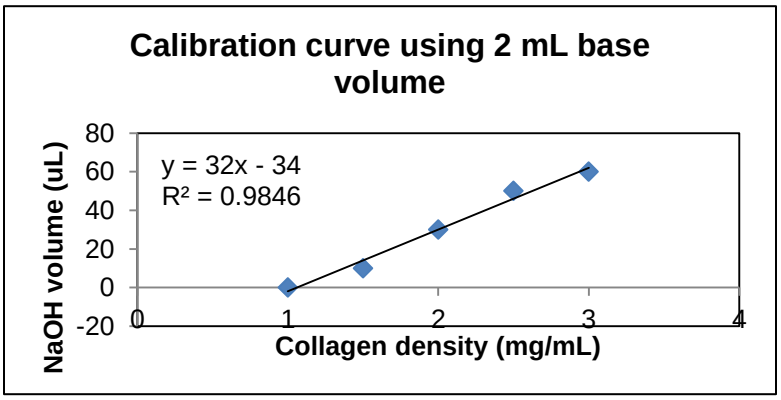

Figure A.1. Calibration curve showing the amount of 0.4 M NaOH that needs to be added to the collagen mixture (2-mL working volume) in order to bring the pH to7.4.

3. Place the collagen mixture onto a 10-mm or 14-mm glass bottom dish.

4. Incubate for at least 2 hours in a humidified 37 ℃ incubator for complete polymerization.

A.2. Collagen hydrogel cell encapsulation protocol

REFERENCES: (Baker, Bonnecaze et al. 2009; Yang and Kaufman 2009)

SUPPLIES

Type I collagen from rat tail (BD Biosciences, Bedford, MA); Respective cell culture medium containing a desired number of cells; 1M HEPES buffer; 0.4 M NaOH; 10-mm or 14-mm glass bottom dish (MatTek Corp., Ashland, MA)

EQUIPMENT

Biological safety cabinet; pH meter; 37 ℃ incubator

PROCEDURE

NOTE: Pre-cool all reagents required for collagen gel fabrication to 4 ℃ before use to prevent any premature collagen gelation upon mixing.

1. Dilute collagen stock solution (8.25 mg/mL to 9.33 mg/mL) with the respective cell culture medium containing a desired number of cells to bring the final concentration to 1.45 or 2.9 mg/mL, as desired. Make 1-mL or 2-mL working volume of the collagen mixture.

2. Add 50 µL of 1 M HEPES buffer and appropriate amounts of 0.4 M NaOH to bring the pH to 7.4 according to previously established calibration curves. An example of such curve is shown in **Figure A.1. (Appendix A.1.).**

3. Place the collagen mixture onto a 10-mm or 14-mm glass bottom dish.

4. Place it in a humidified 37 ℃ incubator. Collagen gel will polymerize and give 3D structural support to the encapsulated cells. In addition, the culture of embedded cells is initiated at this point.

A.3. SEM imaging of collagen hydrogel protocol

SUPPLIES

Type I collagen from rat tail (BD Biosciences, Bedford, MA); Respective cell culture medium; 1M HEPES buffer; 0.4 M NaOH; Liquid nitrogen

EQUIPMENT

SEM (JEOL JSM-6060LV Low Vacuum SEM, JEOL Ltd., Tokyo, Japan); Freeze dryer (VirTis Genesis, Gardiner, NY)

PROCEDURE

1. Make collagen gel solution to be analyzed according to the procedures detailed in **Appendix A.1.**

2. Pour liquid nitrogen directly on top of the fabricated collagen hydrogel to snap freeze it.

3. Quickly move the gel to a pre-cooled (4 ℃) freeze-dryer and freeze dry it for 18 hours.

4. Take SEM images of the prepared gel at 200x magnification, 20 kV, and 10 Pa.

A.4. Collagen hydrogel mechanical characterization protocol

REFERENCES: (Baker, Bonnecaze et al. 2009; Yang and Kaufman 2009)

SUPPLIES

Type I collagen from rat tail (BD Biosciences, Bedford, MA); Respective cell culture medium; 1M HEPES buffer; 0.4 M NaOH

EQUIPMENT

Bohlin C-VOR rheometer (Malvern Instruments, Westborough, MA) with a built-in temperature bath for temperature control

PROCEDURE

NOTE: Pre-cool all reagents required for collagen gel fabrication to 4 ℃ before use to prevent any premature collagen gelation upon mixing.

1. Prepare collagen gel solution according to the procedures detailed in **Appendix A.1.** Make at least 350 µL to analyze.

2. Zero the rheometer (i.e. gap height = 150 µL). Attach a 4° 20-mm cone geometry.

3. Cool the stage to 25 ℃.

4. Place 350 µL of the collagen solution onto the center of the pre-cooled stage.

5. Lower the 4° 20-mm cone geometry down to press the loaded collagen solution. Excess solution around the cone can be trimmed using Kimwipes.

6. Place two small sponges soaked with water on the inside of the solvent trap. Carefully place the solvent trap on top of the loaded collagen gel sample and the cone in order to prevent evaporation during analysis.

7. Open the Bohlin software and adjust settings on the software. Choose oscillatory mode with 1 Hz and 1% strain rate. Also set the software so that rheological measurements will be taken for three consecutive minutes every 20-min intervals.

8. Start the measurement. Raise the temperature of the stage to be 37 ℃ as soon as the test is started. Temperature will be kept at 37 ℃ throughout the remainder of the measurement.

9. Software records moduli data over a 12-hr test period.

A.5. PA gel fabrication protocol

REFERENCES: (Pelham and Wang 1997; Tse and Engler 2010)

SUPPLIES

35 mm glass bottom culture dishes (MatTek Cat # P35G-0-14-C; 14mm microwell)
Circular glass coverslips (Fisher Cat # 12-545-80; 12mm in dia.)
0.1N NaOH
3-aminopropyltrimethoxysilane (keep from moisture)
30 v/v% acrylamide stock solution (light sensitive); from acrylamide powder (Sigma)
3.39g acrylamide in 10 mL solution; density = 1.13 g/cm^3
0.5% glutaraldehyde in PBS (store at 4C)
0.625 mL of 8% stock solution + 9.375 mL of 1x PBS = 10 mL 0.5% solution
3.125 mL of 8% stock solution + 46.875 mL of 1x PBS = 50 mL 0.5% solution
10% APS (make fresh solution every month; keep from light)
1.9g APS in 10mL solution; density = 1.9 g/cm^3
Tetramethylethylenediamine (TEMED)
Acryl/bis-acryl mixture (light sensitive); Fisher Cat# AC33020-1000
50 mM Hepes (pH 8.5)
dichlorodimethylsilane (DCDMS)
DI water

EQUIPMENT

37° incubator; Vortex

PROCEDURE

Day 1:

1. Pipette **200-400 uL of 0.1N NaOH** onto each glass substrate of a glass bottom culture dish. Sufficient NaOH should be added to cover the entire glass surface.

2. Leave it overnight to dry. Evenly distributed crystals should form on the surface by Day 2.

Day 2:

1. Pipette **100 uL of 3-aminopropyltrimethoxysilane** (silanizing agent) onto the NaOH-crystallized glass substrate. Let it dissolve the previously formed NaOH crystals completely.

2. Wait 5 minutes then wash 2x with deionized water.

3. Pipette **200 uL of 0.5% glutaraldehyde in PBS** onto the glass substrate. Let it sit for 30 minutes then wash 2x with deionized water.

4. Remove excess liquid with Kimwipes and leave the dish to air dry completely.

5. Make a PA mixture.

Take **994.5 uL of acryl/bis mixture solution** of a desired concentration.
Add **5uL of 10% APS** (1/200 vol.), **0.5uL of TEMED** (1/2,000 vol.) into the mixture.
Vortex thoroughly.

Acryl % (v/v)	**Bis % (v/v)**	**Elastic modulus**	**Dilution**
4	0.03	0.71 kPa*	Acryl/bis stock = 0.15 mL 30% acryl = 1.143 mL DI water = 8.707 mL
5	0.1	3.48 kPa	Acryl/bis stock = 0.5 mL 30% acryl = 1.033 mL DI water = 8.467 mL
5	0.26	8.75 kPa	Acryl/bis stock = 1.3 mL 30% acryl = 0.020 mL DI water = 8.680 mL
38	2	196 kPa	100% Stock solution (Don't incubate this conc.)

*From literature

Table A.1. Acrylamide/bis-acrylamide concentrations required to make PA gels with a desired elastic modulus.

6. Quickly place **15 uL of acrylamide/bis-acrylamide** mixture onto each glass substrate.

10 uL ~ 70 um thickness (ref: N. Wang Lab)
15 L ~ 75 um thickness (ref: N. Wang Lab)

7. Place a circular coverslip on top of the placed solution then flip over the dish. Keep the dish in the incubator (37C) for 30 minutes. This will ensure that flat gel surface. For 196 kPa PA gels, incubate at room temperature for 10-15 min because the reaction is fast and very exothermic.

Alternatively, place a pre-chlorosilanized coverslip on top of the polymer solution and incubate for 30 minutes.

Chlorosilanization of glass coverslips:

1. Soak the coverslips in DCDMS for 5 minutes.
2. Remove excess DCDMS with KimWipes.
3. Rinse coverslips with DI water for 1 minute.

8. Flip over the dish and add DI water to cover the gel. Just add DI water to cover the gel if chlorosilanized coverslip was used.

9. Carefully remove the circular coverslip with a razor blade.

10. To remove unpolymerized acrylamide, rinse twice in DI water, each time for 5 minutes.

11. Store the gel hydrated in DI water at 4C until needed.

A.6. PA gel surface functionalization protocol

REFERENCES: (Pelham and Wang 1997; Tse and Engler 2010)

SUPPLIES

PA gel
Sulfo-SANPAH (Fisher Scientific, Pittsburgh, PA)
Type I collagen from rat tail (BD Biosciences, Bedford, MA)
50 mM Hepes (pH 8.5)
DI water

EQUIPMENT

UV lamp (365 nm; UVP B-100 High Intensity UV lamp); Vortex

PROCEDURE

1. Take a PA gel and remove liquid with Kimwipes. Careful not to touch the gel itself.

2. Pipette **100 uL of SANPAH** onto each gel surface.
   Sulfo-SANPAH (keep from light) = 50 mg
   DMSO = 500 uL
   50mM HEPES = 50 mL
   *Add DMSO first, then slowly add the HEPES to the sulfo-SANPAH while vortexing.

3. Expose the dish to the UV light (365 nm) at a distance of 2-3 inches for 6 minutes.

Turn on the UV lamp and leave it on for 8 minutes. It takes roughly 30s-1.5min for the lamp to fully turn on.

4. Wash 2x with 50mM HEPES.

5. Repeat #2 – 4.

6. Pipette **200 uL of the desired protein solution** at a desired concentration. Protein solution is made by diluting the stock protein solution in 50 mM HEPES at pH 8.5.

   Collagen conc: 100ug/mL, 40ug/mL, 1 ng/mL

7. Let it activate overnight (> 18 h) at 4C.

8. Remove excess protein solution and rinse 2x with DI water.

9. Prior to seeding cells, sterilize the gel by exposing it to UV for 30 minutes in a sterile hood.

10. Store the gels at 4C until needed. However, using the coated gels right away is recommended. DO NOT store gels for more than 2 weeks.

A.7. PA gel collagen-coating quantification protocol

REFERENCES: (Engler, Bacakova et al. 2004; Engler, Richert et al. 2004)

SUPPLIES

PA gel; Glass bottom culture dishes; 2% BSA in PBS; PBS
Type I collagen from rat tail (BD Biosciences, Bedford, MA)
Primary collagen antibody (Abcam, Cambridge, MA)
Alexa Fluor® 568 secondary antibody (Invitrogen, Carlsbad, CA)

EQUIPMENT

Multiphoton laser scanning microscope (LSM 710; Carl Zeiss AG, Thornwood, NY)

PROCEDURE

1. Deposit known amounts of type I collagen on the glass microwell of glass bottom culture dishes then leave them to dry overnight. Also prepare a blank glass bottom dish to calculate background fluorescence noise to later subtract from the determined fluorescent intensity values.

2. Incubated in 2% BSA in PBS for 45 minutes to block nonspecific binding. When completed, carefully remove 2% BSA in PBS solution with Kimwipes.

3. Incubate with primary collagen antibody (1:200 dilution) for 1 hr. When completed, wash 2x with PBS.

4. Incubate with Alexa Fluor® 568 secondary antibody (1:200 dilution) for 45 minutes. When completed, wash 2x with PBS.

5. Keep samples hydrated in PBS and covered with aluminum foil until ready to image. Image right away to minimize photobleaching.

6. Take collagen-coated PA gels. Wash gels 3x with PBS.

7. Repeat #1-4 with these gels.

8. Take prepared glass bottom culture dishes and PA gels to the microscope to take fluorescent images of the collagen layer.

9. Using ImageJ, compute average fluorescence intensity for all samples.

10. Create a calibration curve to determine the amount of surface-bound collagen.

A.8. AFM force measurement protocol

REFERENCES: (Engler, Bacakova et al. 2004; Engler, Richert et al. 2004)

SUPPLIES

PA gel (collagen-coated and uncoated) samples prepared on microscope slides
Blank glass microscope slide
DNP-S10 silicon nitride AFM probe (Bruker Corp., Camarillo, CA)
DI water; Hydrophobic pen

EQUIPMENT

MFP-3D AFM (Asylum Research, Santa Barbara, CA)

PROCEDURE

Get ready:

1. Turn on Igor software. Select 'contact mode'.
2. Turn Laser on.
3. Turn light source on.

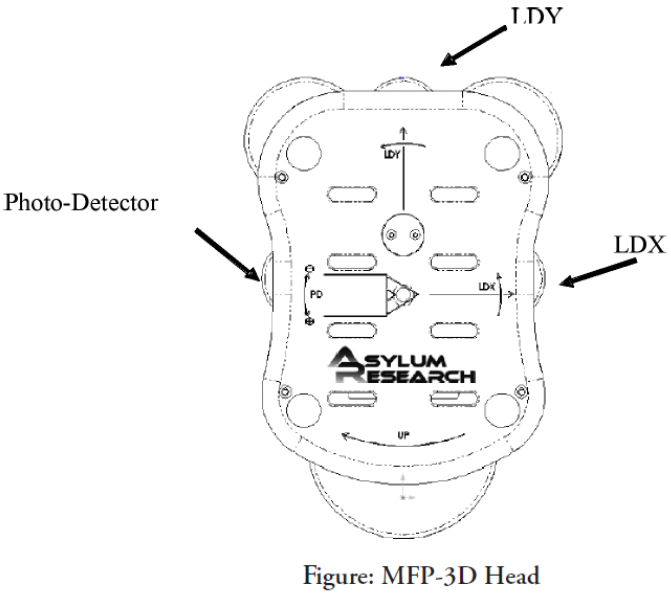

Figure A.2. A top-down view of the AFM head. Photo-Detector knob adjusts deflection. LDY and LDX knobs control the laser position in y- and x-directions, respectively. Camera control knobs are located near the LDY knob. The big wheel at the front end lifts the head up or down.

NOTE: The head is very heavy and needs to be handled with caution. Also pay attention to the cables attached to the head because it is easy to snap off the cables.

1. Cantilever Calibration

NOTE: Always make sure the head is level! The bubble of the bubble top should be at the center, slightly to the front.

NOTE: RED = Extension; BLUE = Retraction

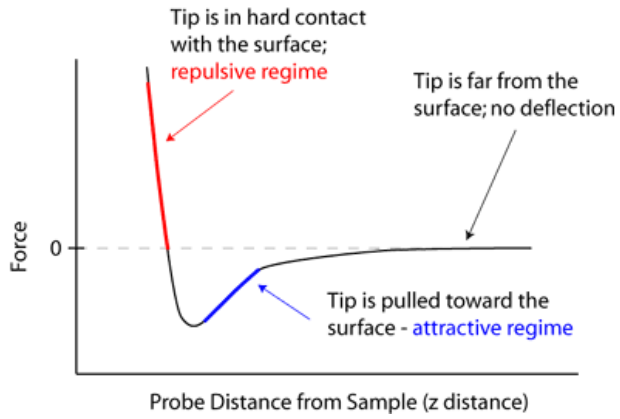

Figure A.3. An example of a force-indentation curve generated with AFM.

1. Place a clean bare glass microscope slide on the sample holder.
    a. Draw a hydrophobic circle on the glass slide before loading.
2. **Mount the probe** on the probe holder.
    a. The probe should not be too far back or too far out.
    b. It should be about 1-1.5 mm away from the end of the clear probe mount.
    c. From the side, the probe sits at a slightly slanted upward angle.
    d. Once ready, place the probe holder into the AFM head.
3. **Laser Alignment.**
    a. Find the laser spot and place it at the end of the tip to be used.
    b. Adjust to get maximum sum signal.
    c. Adjust deflection to zero.
    d. Let it stand for a few minutes if deflection fluctuates. Deflection may be unstable if there are charges on the surface or huge adhesion forces near the surface due to a water layer on a rainy day, etc.
4. **Check thermal peaks** under the thermal tab. Verify that a correct peak exits within the manufacturer specified drive frequency range.
5. **Force calibration.**
    a. 'Engage'. Zero the deflection then bring down the head until the tip touches the surface, with a clicking sound from the software. Adjust Z voltage to be at zero.
    b. Adjust settings: Trigger Channel
        i. Trigger channel: DefInVols
        ii. Positive slope

iii. Relative
iv. For soft cantilevers, change Force distance = 10 um
Trigger point = 3 V

c. Hit 'Single Force'. It should generate a single force curve. Hit it one more time if the tail is too long or is at an angle.
i. Bring out cursors with "Control + i"
ii. Locate them on the tail
iii. Set sensitivity = Virtual Deflection
iv. Zoom into the linear region of the curve.
v. Place the cursors on the linear region. The cursors should move together if you move along the curve with arrow keys.
vi. Set sensitivity = DeftInVols
vii. Check AmpInVols to see if it's between 30 and 60. Write down this number. Even if this number is greater than 60, it is okay as long as the calibrated spring constant is close to the nominal spring constant.

6. **Thermal calibration**.
a. Physically lift head up from sample (turn the knob 10x). Deflection should change as the head is moved up; however, it should stay stable.
b. Do thermal.
c. Fit to the peak corresponding to the specified drive frequency of the tip.
d. 'Try fit' until little to no change in spring constant. Record the spring constant.
e. Check AmpInvols. Record this number.
7. **Transition to Liquid Mode.**
a. Carefully lift head up.
b. Add a few drops of water on the probe and around it.
c. Pipette some DI water onto the pre-drawn hydrophobic circle on glass slide.
d. Place the head down carefully. You can see from the camera that the tip is now submerged in water.
e. Make sure there are no air bubbles on the tip!
f. Adjust deflection and laser position to get good sum signal.
g. Wait 5 minutes or more for deflection to stabilize.
h. Do 'Single force' to create a force curve. It should look similar to the force curve in air mode.
i. Check AmpInVols. It may shift quite a bit. Record this number. You will use this number for any subsequent data analysis.

<u>2. Force measurements of the gel samples</u>

1. Make sure head is level. Also, disengage head so that the tip won't be touching the sample once the sample is loaded. The tip will get destroyed if head is too close to sample.
2. **Load sample.**
NOTE: Always do the stiff substrates first, then move to softer ones to minimize damage to AFM probes.
a. Bring head down so that the tip is fully immersed in liquid.
b. Wait about 5 minutes for deflection to stabilize.
c. Engage the tip and find the surface, then withdraw.
d. Adjust force measurement settings.

i. Velocity = 1 µm/s
ii. Indentation depth = 2 µm

e. Hit Single force.
f. Hit withdraw.
g. Move the stage in x- and/or y-directions to locate the AFM probe on different spots of the loaded samples. Repeat e-f. (N = at least 15 per sample)

8. When done, lift up the head.
9. Remove the sample. Load another and repeat as needed.

3. Saving the data files

1. Force tab -> 'Review'.
2. Select force curves to be saved.
3. Modify x- and y-offset.
4. Menu on the very top of IGOR Pro: Select Data -> Save waves -> Save as delimited text.
5. Find the folder where the force data is saved.
6. Select the correct files to be imported then hit 'Do it'. For Hertz force calculations, only the 'Ext' files are required. (Red = extension; Blue = retraction).

4. Clean-up

1. Remove the AFM probe and clean the probe holder with an air spray or nitrogen spray to remove any liquid. Put the holder back into the head.
2. Put everything back to where it was.
3. Keep the AFM chamber closed.

APPENDIX B: CELL CULTURE AND ANALYSIS PROTOCOLS

B.1. HSC isolation protocol

REFERENCES: (Liang, Jansen et al. 2007)

SUPPLIES

Animals to sac:
WT Jax C57B6 mouse strain: 1 mouse

FACS Antibodies:
Lineage cocktail [CD5, CD45R (B220), CD11b, Anti-Gr-1 (Ly-6G/C), 7-4, Ter-119]
Sca-1
c-Kit
*All antibodies are purchased from eBiosciences.

Materials:
70% ethanol solution
Surgical tools – scissors, tweezers
Timer; Pen; Petri dish
Vacuum chamber – vacuum flask, plastic tubing, and glass pipettes for aspiration
Pre-cooled reagents – ACK lysis buffer, separation buffer, PBS/2%FBS (at 4°C)
PBS/2%FBS: 20 mL for temporarily storing femurs and tibias
40 mL for crushing and filtering bones
35 mL for quenching after lysis step
10 mL for miscellaneous use
40 μm cell strainer

EQUIPMENT
Biological safety cabinet; Vortex; Centrifuge; Flow cytometer (Analyzer or sorter)

PROCEDURE

Isolation of BM cells from mouse:

1. Sacrifice mouse via CO_2inhalation. (Make sure to bring 70% ethanol solution, surgical scissors and tweezers, gloves, and a pen to the animal facilities lab.)
2. Remove tibia and femur (entire length incl. head of femur) from both sides. Remove any attached muscle (via gentle Kim-wipe rubbing). Keep cleaned bones in PBS+2%FBS.
3. Place bones into (cleaned/autoclaved) mortar with some PBS+2%FBS. Gently crush the bones using a pestle. Do not grind with continuous motion in the x direction: instead, use a gentle up-and-down motion.
4. Pour PBS+2%FBS + ground bones through a 40μm cell strainer into a 50ml conical tube. Add more PBS+2%FBS and grind. Repeat until 40mL PBS+2%FBS is used up. While doing this, also make sure to rinse mortar and pestle once in a while to collect all cells.
5. Spin down: 1400 rpm, 5 minutes, 4°C. Aspirate supernatant.

6. Resuspend cells in 5ml ACK lysis buffer, vortex well. Let stand 5 min (no more!) on ice. Quench with 35ml PBS+2%FBS.
7. Spin down: 1400 rpm, 5 minutes, 4°C. Aspirate supernatant.
8. Resuspend in PBS+2%FBS in 1mL. Count live cells from a 10µL aliquot (+10µL Trypan blue) with a hemocytometer. For easy cell counting, dilute the cell suspension at least by a factor of 5.

	WT
Avg. count (hemocytometer grid)	
Total # cells/mL	

FACS analysis/sorting for further enrichment in LSK population: All steps done on ice

1. Add Fc receptor blocking antibody to achieve 0.5 µg/mL concentration. Sit 10' on ice.
2. Spin down: 1400 rpm; 5 minutes; 4°C. Aspirate the supernatant.
3. Resuspend in 1mL PBS+2% FBS.

   For first time sorting or when compensation needs to be updated, divide the BM suspension in volumes of 300µL containing 250,000 cells to generate control samples listed in the following table.

#	**FACS Tube**	**Contents**
1	Unstained control	WBM
2	PI control	WBM, PI
3	APC control	WBM, Sca-1-APC
4	PE control	WBM, c-kit-PE
5	FITC control	WBM, Lin-FITC
6	Stained sample	WBM, PI, c-kit-PE, Sca-1-APC, Lin-FITC

4. Add antibody cocktails (Lin, Sca-1, and c-Kit); Sit 20' on ice.

Lin cocktail	**Dilution**
CD5	1:200
B220	1:300
Mac-1	1:320
CD8a	1:200
Gr-1	1:350
Ter-119	1:320

Note) Dilutions when antibodies are at 0.5 mg/mL.

Antibody cocktail	Amount
Lin cocktail	7 µL
Sca-1-PE	7 µL
c-kit-APC	7 µL
TOTAL	21 µL

5. Add 100 µL of PI stock solution into 10mL PBS+2%FBS to make a PI working solution. Add 20µL of the PI working solution to the cells. Mix. Quench with 2mL PBS/2% FBS right away because PI staining is instantaneous.
6. Spin down: 1400 rpm, 5 minutes, 4^{o}C.
7. Resuspend in 1.5mL PBS+2% FBS; pipette up/down, vortex to generate single cell suspension.
8. Filter into new tubes. Use polypropylene tubes to minimize cell loss through cells attaching to the tubes. Polypropylene is superior to polystyrene.
9. Flow analysis/sorting on each population.

B.2. Cell viability assay protocol

SUPPLIES

Hydrogel samples with live cells
LIVE/DEAD Cell Viability Assay kit (Invitrogen, Carlsbad, CA)

EQUIPMENT

Fluorescence microscope (Leica DMI4000, Leica Microsystems GmbH, Wetzlar, Germany)

PROCEDURE

1. Make a 500 µL working solution in PBS.
    a. Add 1 µL ethidium homodimer-1, red
    b. Add 0.6 µL calcein, green

2. Add 100 µL to each glass bottom culture dish.

3. Incubate for 15 minutes at 37 ℃.

4. Image with a fluorescence microscope. Live cells are stained green and dead cells are stained red.

B.3. Fixed cell staining protocol

SUPPLIES

Samples with cells
3.7% formaldehyde
0.1% Triton X100
ITsignal FX (Invitrogen, Carlsbad, CA)
DAPI (Invitrogen, Carlsbad, CA)
Alexa Fluor® 488-phalloidin (Invitrogen, Carlsbad, CA)
Prolong Gold® (Invitrogen, Carlsbad, CA)

EQUIPMENT

Multiphoton laser scanning microscope (LSM 710; Carl Zeiss AG, Thornwood, NY)

PROCEDURE

NOTE:
- All procedures performed at room temperature.
- 100 uL solution is used at each step unless otherwise stated.
- Leave the sample in PBS for about a minute per rinse.
- Use Kimwipes to remove excess liquid for the rinsing step.
- Do not use BSA with ITsignal FX as it may interfere with the effectiveness of the product.

1. Fix sample in 3.7% formaldehyde for 15 minutes.
   Wash sample 3x with PBS.

2. Incubate sample in 0.1% Triton X100 in PBS for 15 minutes.
   Wash sample 3x with PBS.

3. Add 2 drops (~100uL) of ITsignal FX and incubate for 30 minutes. IT signal enhances sample fluorescence signal while reducing background noise.
   Wash sample 1x with PBS.

4. Dilute 5uL of methanolic stock solution (Alexa Fluor 488-phalloidin) into 200uL PBS/ITSignal FX (150uL plus a drop of ITSignal FX) for each sample. Incubate sample in this solution for 30 minutes.

5. Prepare DAPI solution (1:800 dilution). When 25 minutes of incubation has passed (5 min before completion), place the DAPI solution to the sample.

6. After full 30 min of incubation, wash sample 3x with PBS.

7. To minimize photobleaching, add a drop or two of Prolong Gold antifade reagent. Cure for 24 hours at room temperature before storing at 4 ℃.

B.4. ImageJ: Cell spread area calculation protocol

SUPPLIES

Images of cells to be analyzed (either F-actin images or phase contrast images)
ImageJ (Free download available from online)

EQUIPMENT

Fluorescence or light microscope with 40x or higher magnification

PROCEDURE

1. Open either a confocal image (fluorescence) or a phase contrast image. The image should have a scale bar.

2. **Analyze -> Set scale.** Usually comes to 6.3 pixels per unit OR 63 pixels for 10 microns, but will vary depending on the picture size and magnification used.

Image enhancement (Necessary for phase contrast images only): Steps #3-5

3. **Process -> Smooth OR Sharpen**, depending on which one gives clearer, more defined edges of the objects of interest.

4. **Process -> Enhance contrast.** Set it to 0.7%. If this doesn't give defined edges, try 0.001%.

5. **Image -> Adjust -> Brightness/Contrast.**
   Image -> Adjust -> Color balance (All colors).
   Image -> Adjust -> Threshold color -> Hue settings reduces background noise quite well. Adjust these settings until more defined edges are obtained.

6. **Image -> Type -> 8-bit** to make it a black & white image.

7. **Image -> Adjust -> Threshold.** Adjust until the objects of interest stand out and the background noise level is minimized. Hit 'Apply'.

8. **Process -> Binary -> Make binary.** A pop up window will appear. Do this once more. The pop up window will not appear this time.

9. Using the **wand tool,** click an object of interest. If it has holes to fill, then fill them by clicking 'Cntl+F'. Fill until a uniformly filled object is selected.

10. **Analyze -> Set measurements -> Check 'Area' and 'Perimeter'**.

11. **Analyze -> Analyze particles** -> Adjust range (usually 10 – Infinity works. Increase/Decrease depending on expected cell size). Show ‘Outlines’.

12. Continue analyzing until only one object (or objects of interest) is identified. That is, objects of interest being identified as multiple particles is NOT good. One cell should be identified as one particle. Record computed area and perimeter for further calculations.

13. Save the thresholded image for record.

REFERENCES

Agliano, A. M., C. Santangelo, et al. (2000). "On chromosomal instability: what is the karyotype of your 32D Cl3 cell line?" Blood **95**(11): 3636-3637.

Baker, E. L., R. T. Bonnecaze, et al. (2009). "Extracellular Matrix Stiffness and Architecture Govern Intracellular Rheology in Cancer." Biophysical Journal **97**(4): 1013-1021.

Beningo, K. A., C.-M. Lo, et al. (2002). Flexible polyacrylamide substrata for the analysis of mechanical interactions at cell-substratum adhesions. Methods in Cell Biology, Academic Press. **Volume 69:** 325-339.

Bersenev, A., C. Wu, et al. (2008). "Lnk controls mouse hematopoietic stem cell self-renewal and quiescence through direct interactions with JAK2." J Clin Invest **118**(8): 2832-2844.

Bonnet, D. and J. E. Dick (1997). "Human acute myeloid leukemia is organized as a hierarchy that originates from a primitive hematopoietic cell." Nat Med **3**(7): 730-737.

Can, A. (2008). "Haematopoietic stem cells niches: Interrelations between structure and function." Transfusion and Apheresis Science **38**(3): 261-268.

Carl, P. and H. Schillers (2008). "Elasticity measurement of living cells with an atomic force microscope: data acquisition and processing." Pflügers Archiv European Journal of Physiology **457**(2): 551-559.

Chowdhury, F., S. Na, et al. (2009). "Material properties of the cell dictate stress-induced spreading and differentiation in embryonic stem cells." Nat Mater **9**(1): 82-88.

Discher, D. E., D. J. Mooney, et al. (2009). "Growth factors, matrices, and forces combine and control stem cells." Science **324**(5935): 1673-1677.

Domke, J. and M. Radmacher (1998). "Measuring the elastic properties of thin polymer films with the atomic force microscope." Langmuir **14**(12): 3320-3325.

Ehninger, A. and A. Trumpp (2011). "The bone marrow stem cell niche grows up: mesenchymal stem cells and macrophages move in." The Journal of Experimental Medicine **208**(3): 421-428.

Engler, A., L. Bacakova, et al. (2004). "Substrate compliance versus ligand density in cell on gel responses." Biophys J **86**(1 Pt 1): 617-628.

Engler, A. J., L. Richert, et al. (2004). "Surface probe measurements of the elasticity of sectioned tissue, thin gels and polyelectrolyte multilayer films: Correlations between substrate stiffness and cell adhesion." Surface Science **570**(1-2): 142-154.

Engler, A. J., S. Sen, et al. (2006). "Matrix elasticity directs stem cell lineage specification." Cell **126**(4): 677-689.

Gavara, N. and R. S. Chadwick (2010). "Noncontact microrheology at acoustic frequencies using frequency-modulated atomic force microscopy." Nat Meth **7**(8): 650-654.

Holst, J., S. Watson, et al. (2010). "Substrate elasticity provides mechanical signals for the expansion of hemopoietic stem and progenitor cells." Nat Biotech **28**(10): 1123-1128.

Jan, M., M. P. Chao, et al. (2011). "Prospective separation of normal and leukemic stem cells based on differential expression of TIM3, a human acute myeloid leukemia stem cell marker." Proc Natl Acad Sci U S A **108**(12): 5009-5014.

Kandow, C. E., P. C. Georges, et al. (2007). Polyacrylamide Hydrogels for Cell Mechanics: Steps Toward Optimization and Alternative Uses. Methods in Cell Biology. W. YuLi and E. D. Dennis, Academic Press. **Volume 83:** 29-46.

Li, C., C. J. Lee, et al. (2009). "Identification of human pancreatic cancer stem cells." Methods Mol Biol **568**: 161-173.

Liang, Y., M. Jansen, et al. (2007). "The quantitative trait gene latexin influences the size of the hematopoietic stem cell population in mice." Nat Genet **39**(2): 178-188.
lls.org (2011). Leukemia & Lymphoma Society: Fighting Blood Cancers.
Lutolf, M. P., R. Doyonnas, et al. (2009). "Perturbation of single hematopoietic stem cell fates in artificial niches." Integrative Biology **1**(1): 59-69.
Mahaffy, R. E., C. K. Shih, et al. (2000). "Scanning probe-based frequency-dependent microrheology of polymer gels and biological cells." Physical Review Letters **85**(4): 880-883.
Pajerowski, J. D., K. N. Dahl, et al. (2007). "Physical plasticity of the nucleus in stem cell differentiation." Proceedings of the National Academy of Sciences **104**(40): 15619-15624.
Passegue, E., C. H. Jamieson, et al. (2003). "Normal and leukemic hematopoiesis: are leukemias a stem cell disorder or a reacquisition of stem cell characteristics?" Proc Natl Acad Sci U S A **100 Suppl 1**: 11842-11849.
Patel, P. N., C. K. Smith, et al. (2005). "Rheological and recovery properties of poly(ethylene glycol) diacrylate hydrogels and human adipose tissue." Journal of Biomedical Materials Research Part A **73A**(3): 313-319.
Ped-Onc.org. (2011). "Leukemia." Retrieved Nov 16, 2011, from http://www.ped-onc.org/diseases/leuk.html.
Pelham, R. J. and Y. L. Wang (1997). "Cell locomotion and focal adhesions are regulated by substrate flexibility." Proceedings of the National Academy of Sciences of the United States of America **94**(25): 13661-13665.
Radmacher, M. (1997). "Measuring the elastic properties of biological samples with the AFM." Ieee Engineering in Medicine and Biology Magazine **16**(2): 47-57.
Raub, C. B., V. Suresh, et al. (2007). "Noninvasive assessment of collagen gel microstructure and mechanics using multiphoton Microscopy." Biophysical Journal **92**(6): 2212-2222.
Ross, J. and L. H. Li (2009). "HSC mobilization: new incites and insights." Blood **114**(7): 1283-1284.
Rowlands, A. S., P. A. George, et al. (2008). "Directing osteogenic and myogenic differentiation of MSCs: interplay of stiffness and adhesive ligand presentation." American Journal of Physiology - Cell Physiology **295**(4): C1037-C1044.
Saha, K., A. J. Keung, et al. (2008). "Substrate Modulus Directs Neural Stem Cell Behavior." Biophysical Journal **95**(9): 4426-4438.
Schneider, A., G. Francius, et al. (2005). "Polyelectrolyte Multilayers with a Tunable Young's Modulus: Influence of Film Stiffness on Cell Adhesion." Langmuir **22**(3): 1193-1200.
Singh, S. K., I. D. Clarke, et al. (2003). "Identification of a cancer stem cell in human brain tumors." Cancer Res **63**(18): 5821-5828.
Taussig, D. C., F. Miraki-Moud, et al. (2008). "Anti-CD38 antibody-mediated clearance of human repopulating cells masks the heterogeneity of leukemia-initiating cells." Blood **112**(3): 568-575.
Thakar, R. G., M. G. Chown, et al. (2008). "Contractility-Dependent Modulation of Cell Proliferation and Adhesion by Microscale Topographical Cues." Small **4**(9): 1416-1424.
Tse, J. R. and A. J. Engler (2010). "Preparation of hydrogel substrates with tunable mechanical properties." Curr Protoc Cell Biol **Chapter 10**: Unit 10 16.

Valtieri, M., D. J. Tweardy, et al. (1987). "Cytokine-Dependent Granulocytic Differentiation - Regulation of Proliferative and Differentiative Responses in a Murine Progenitor-Cell Line." Journal of Immunology **138**(11): 3829-3835.

Weissman, I. L. and J. A. Shizuru (2008). "The origins of the identification and isolation of hematopoietic stem cells, and their capability to induce donor-specific transplantation tolerance and treat autoimmune diseases." Blood **112**(9): 3543-3553.

Wilson, A. and A. Trumpp (2006). "Bone-marrow haematopoietic-stem-cell niches." Nat Rev Immunol **6**(2): 93-106.

Yang, Y. L. and L. J. Kaufman (2009). "Rheology and Confocal Reflectance Microscopy as Probes of Mechanical Properties and Structure during Collagen and Collagen/Hyaluronan Self-Assembly." Biophysical Journal **96**(4): 1566-1585.

Yannas, I. V., D. S. Tzeranis, et al. (2010). "Biologically active collagen-based scaffolds: advances in processing and characterization." Philos Transact A Math Phys Eng Sci **368**(1917): 2123-2139.

Zon, L. I. (2008). "Intrinsic and extrinsic control of haematopoietic stem-cell self-renewal." Nature **453**(7193): 306-313.